Geophys. J. R. astr. Soc. (1980) **61**, 489–517

Eocambrian–Cambrian palaeomagnetism of the Armorican Massif, France

Jonathan T. Hagstrum and Rob Van der Voo *Department of Geology and Mineralogy, The University of Michigan, Ann Arbor, Michigan 48109, USA*

Bernard Auvray and Norbert Bonhommet *Centre Armoricain d'Etude Structurale des Socles, L.P. 466 of CNRS, Institut de Géologie, Av. du Général-Leclerc, 35042 Rennes-Cedex France*

Received 1979 September 17; in original form 1979 April 23

Summary. In an attempt to clarify pre-Hercynian continental configurations, palaeomagnetic data were collected from the spilites de Paimpol (640 ± 12 Myr), the diorite de St Quay (583 ± 40 Myr), the gabbro de Keralain (undated), the granite de Porz-Scarff (557 ± 16 Myr), the rhyolitic ignimbrites of Lézardrieux (546 ± 8 Myr) and the rhyolites de St Germain-le-Gaillard (undated) from the unmetamorphosed to slightly metamorphosed Eocambrian–Cambrian terranes of the Domnonean Domain of northern Brittany and north-western Normandy.

Upon stepwise thermal and/or alternating field demagnetization and using vector subtraction, the spilites de Paimpol yield a characteristic direction with declination (D) = 226.4°, inclination (I) = – 15.7°. Local remagnetization by microgranite dykes (approximately 560 Myr old) produced a direction of $D = 235.1°$, $I = +63.4°$. The diorite de St Quay exhibits multivectorial behaviour revealing a characteristic component of $D = 31.2°$, $I = -2.3°$, and a secondary component of $D = 299.9°$, $I = +38.2°$. The gabbro de Keralain shows a characteristic component ($D = 290.9°$, $I = 41.4°$) similar to the diorite's secondary component, and gives a secondary component of $D = 221.0°$, $I = +55.8°$. This secondary component of the gabbro appears again as the characteristic (although somewhat scattered) directions of the granite de Porz-Scarff. Thus, the gabbro may be relatively dated as having been magnetized before the intrusion and cooling of the granite (557 ± 16 Myr) and after that of the diorite (583 ± 40 Myr). The data from the rhyolites are the least certain because of ambiguities in the radiometric dating and uncertain bedding corrections, but they contain directions near to those of the granite and the microgranite dykes, all believed to be of the same episode of acidic volcanism.

The trend in palaeomagnetic poles from the Armorican Massif for the Eocambrian–Cambrian corresponds well with coeval data from the southern United Kingdom and Czechoslovakia (Bohemian Massif), suggesting that a single continental mass, Armorica, contained all three areas. A comparison with poles from Gondwanaland also shows a remarkable agreement and suggests a period of coherent movement during the Latest Precambrian and the Cambrian for Armorica and Gondwana, followed by later separation. This leaves the Armorica plate as a separate continental unit at the outset of the Caledonian orogeny later in the Palaeozoic.

Introduction

The juxtaposition of different Lower Palaeozoic faunal realms and the separation of other similar assemblages by the width of the Atlantic Ocean was first recognized by J. T. Wilson (1966) as strong evidence for a pre-Permian proto-Atlantic Ocean. Since then a more complex tectonic picture of the major Palaeozoic orogenies and continental motions is emerging for the Atlantic-bordering continents. Several Lower Palaeozoic oceans, which disappeared along the sites of continental suturing, have been proposed, and associated with the closure of each ocean and consequent continental collision is an orogeny (McKerrow & Ziegler 1972; Dewey & Kidd 1974). Of primary interest for this paper are the fundamental tectonic settings of the Cadomian, Caledonian and Hercynian orogenies, each possibly the result of the closure of oceans between the combined Baltic Shield–Russian Platform, Central Europe, cratonic North America, and Gondwanaland.

Of these, the Hercynian orogeny is especially enigmatic. The Hercynian orogenic belt contains no pronounced tectonic characteristics of either a predominantly collisional or subduction event. Thus, an entire spectrum of hypotheses between these two endpoints has arisen in order to explain the Hercynian orogeny in plate tectonic terms (e.g. collision: Johnson 1973, 1974; Dewey & Burke 1973; Burrett 1972; Burne 1973; subduction: Nicolas 1972; Floyd 1972; microplates: Laurent 1972; Riding 1974; Badham & Halls 1975; Lorenz 1976). Most of these models, however, are for the Hercynian orogeny proper, e.g. the Bretonian, Sudetian, Asturian and minor folding phases of Stille (1924), thought to range in age between Late Devonian (*c.* 360 Myr) and Late Carboniferous (*c.* 280 Myr). Early and Middle Palaeozoic situations are more difficult to reconstruct due to the unclear continuity between individual Hercynian Massifs and also because of some possible overprinting by the Hercynian orogeny (Poland, Belgium) in the Caledonian belts.

Important to the resolution of the true nature of the Hercynian orogeny would be an accurate description, at least in latitudinal terms, of the relative positions of the continental pieces involved. Such information is available through palaeomagnetic study. Palaeomagnetic data for northern and eastern Europe as well as the North American and Gondwana continents enable a general framework before the orogeny to be established (e.g. French 1976; Irving 1977; Morel & Irving 1978). It must be noted, however, that data for the Lower Palaeozoic are scarce and until recently for any portion of Hercynian Europe extremely rare. Late Devonian redbeds from Normandy and remagnetized Cambro-Ordovician redbeds and trachyandesites from Normandy and Brittany have been sampled by Jones, Van der Voo & Bonhommet (1979). The resulting data imply no separation between Hercynian and stable Europe from the Late Devonian to Early Carboniferous, whereas a comparison of their Armorican poles with those for the Gondwana continents suggests an intervening ocean. The closure of this ocean and collision of Gondwanaland with Europe may have occurred as a result of subduction at a zone to the south of Hercynian Europe (Jones *et al.* 1979). Our study, subsequent to those of Jones (1978) and Jones *et al.* (1979), was undertaken to further the understanding of the pre-Hercynian continental configurations and what effect it may have on the orogeny itself.

Radiometrically dated volcanic units were selected for sampling from the Armorican Massif in western France, accompanying radiometric dating already underway at the University of Rennes, France. The Armorican Massif was chosen for its exposure of unmetamorphosed to only moderately metamorphosed Early Palaeozoic rocks, particularly in the northern Domnonean and Mancellian Domains (Cogné 1974). The rocks studied are the spilites de Paimpol and younger intrusive dykes, the diorite de St Quay, the gabbro de Keralain (undated), the granite de Porz-Scarff, the rhyolitic ignimbrites of Lézardrieux and the rhyolites de St Germain-le-Gaillard (undated). The oldest rocks are the spilites (Rb/Sr whole rock isochron age of 640 ± 12 Myr), whereas the youngest formation is thought to be the rhyolitic ignimbrites of Lézardrieux (Rb/Sr whole rock isochron age of 546 ± 8 Myr).

The dates imply Late Precambrian and Early Cambrian ages, according to the time-scale of Van Eysinga (1975). Geographically, all rock units studied except for the rhyolites de St Germain-le-Gaillard come from a tectonic domain to the west of the Baie de St Brieuc, including the region of the Trégor (inset, Fig. 1). This area is thought to have been a relatively coherent tectonic unit since at least the Cadomian orogeny, i.e. since at least Latest Precambrian time (Cogné 1971). Sequential palaeomagnetic results might, therefore, provide us with a segment of the apparent polar wander path for this unit, that can then be compared with apparent polar wander paths of other continental blocks. The fact that palaeomagnetic poles for the Cambrian period are rare for any continent makes conclusions

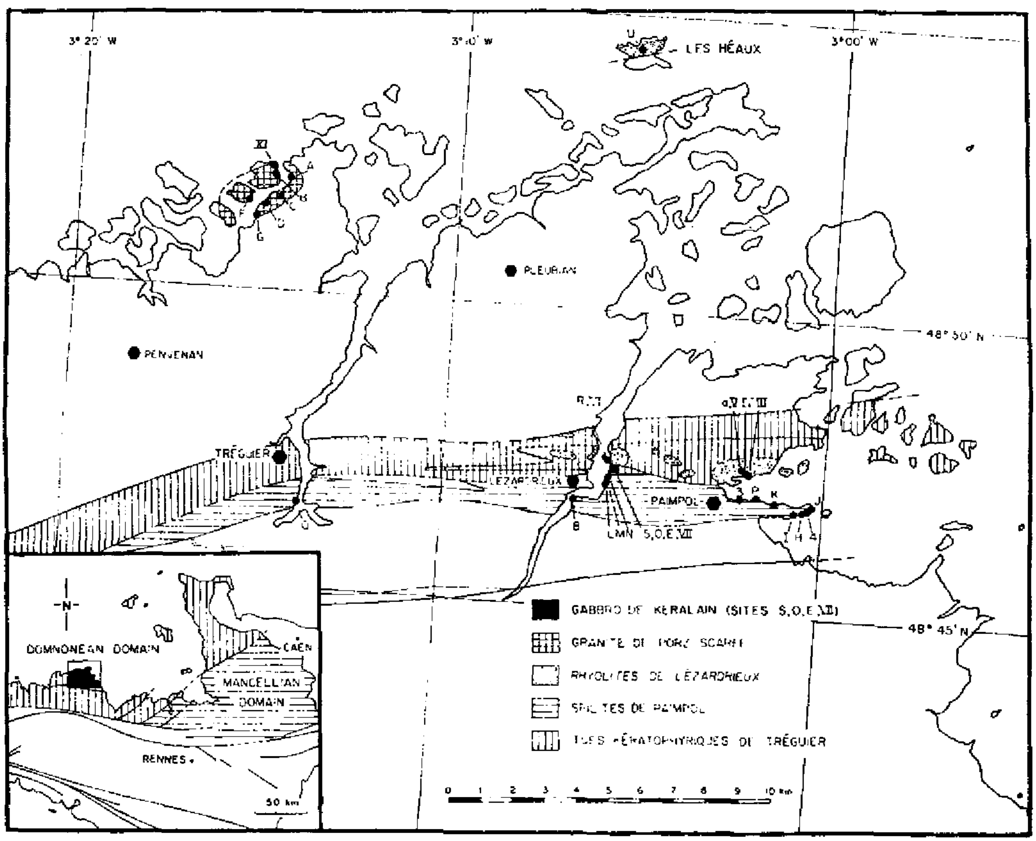

Figure 1. Sampling localities in the Trégor area of the Domnonean Domain, Brittany, with schematic geological features (after Pruvost, Waterlot & Delattre 1966 and Auvray, Lefort & Monnier 1976a). Inset after Cogné (1974).

reached from such a comparison tentative at best. Substantiation for these tentative assessments must await other results (e.g. for the Cambrian of the Baltic Shield–Russian Platform, Gondwanaland, North America, as well as other areas in the Caledonian and Hercynian belts). A palaeomagnetic approach to such problems as mentioned above is promising, but in its early stages, not unlike the first palaeomagnetic evidence obtained from North America and Europe for the post-Triassic opening of the Atlantic Ocean (e.g. Runcorn 1962).

Field and laboratory techniques

Samples were collected in the field both by drilling and handsampling. The majority of samples (62 per cent) were taken as handsamples. Those drilled in the field were oriented by

Table 1. Site means and group means.

Site	N/N_0	Strike/dip	Decl./incl.	k_2	α_{95}	Pole position	k_2/k_1
Spilites de Paimpol							
HFH	5/5	88/63	[226.3/-27.8]	1.6	84.9	-- ---	
3	5/5	73/75	231.1/-21.5	50.0	10.9	33.5 S, 290.8 E	
HFK	3/5	73/64	212.6/-24.6	24.8	25.3	45.2 S, 308.8 E	
HFP	7/7	91/59	220.3/-19.3	34.9	10.4	38.7 S, 302.3 E	
HFL	2/5	71/63	242.1/+ 1.7	22.5	55.4	17.2 S, 289.1 E	
HFM	4/7	60/60	223.3/-11.1	12.5	27.1	33.4 S, 302.0 E	
HFN	3/5	52/61	214.8/- 2.7	14.5	33.6	34.0 S, 313.4 E	
HFQ	7/7	83/63	241.5/-30.1	16.1	15.5	30.8 S, 277.6 E	
Mean	7/8		226.4/-15.7	24.6	12.4	33.8 S, 297.2 E	0.66
Microgranite dykes and remagnetized spilite flows							
HFHd	4/4		[340.1/+59.7]	2.9	65.3	-- ---	
HFIf	4/5		285.3/+71.1	13.7	25.7	46.0 N, 305.4 E	
HFId	3/6		228.6/+54.2	2.1	51.5	2.5 N, 317.9 E	
4	4/4		220.1/+59.4	16.0	23.7	5.7 N, 327.4 E	
HFJf	6/6		238.3/+51.9	8.1	25.0	6.4 N, 310.8 E	
HFJd	4/5		241.0/+60.4	14.9	25.1	14.8 N, 314.2 E	
8	3/4		205.7/+74.0	26.3	24.5	20.9 N, 343.5 E	
Mean	6/7		235.1/+63.4	35.2	11.4	16.2 N, 310.3 E	
Diorite de St.Quay (Characteristic directions)							
HFT	11/14		29.5/- 7.2	68.6	5.6	31.9 N, 141.9 E	
HFW	5/10		30.0/+ 0.3	17.5	18.8	35.0 N, 139.5 E	
HFV	5/5		34.7/+ 3.5	42.4	11.9	34.4 N, 133.5 E	
HFX	5/5		31.2/- 0.3	104.4	7.5	34.3 N, 138.4 E	
HFY	5/5		30.7/- 5.0	16.0	19.7	32.3 N, 140.0 E	
HFZ	4/4		30.7/- 9.8	56.9	10.2	32.8 N, 139.7 E	
HFII	5/5		31.8/+ 2.7	31.8	13.8	35.4 N, 142.6 E	
Mean	7/7		31.2/- 2.3	226.2	4.0	33.7 N, 138.6 E	

Table 1 – *continued*

Site	N/N_0	Strike/dip	Decl./incl.	k_2	α_{95}	Pole position	k_2/k_1
Diorite de St.Quay (Secondary direction)							
HFT	8/14		303.4/+44.5	20.7	12.5	41.1 N, 261.1 E	
HFW	3/10		297.9/+39.7	14.7	33.4	35.0 N, 262.2 E	
HFY	1/5		298.8/+30.4	-	-	31.1 N, 256.3 E	
Mean	3/7		299.9/+38.2	116.5	11.5	37.6 N, 262.1 E	
Gabbro de Keralain (Characteristic direction)							
VIII	5/5		288.1/+42.6	45.8	11.4	30.0 N, 271.1 E	
HFO	5/5		292.0/+41.6	40.0	12.2	32.1 N, 267.6 E	
HFS	27/27		292.5/+40.1	53.1	3.9	31.6 N, 266.3 E	
Mean	3/3		290.9/+41.4	1363	3.3	31.3 N, 268.3 E	
Gabbro de Keralain (Secondary direction, 9 samples)							
	9/37		221.0/+55.8	12.0	15.5	2.6 N, 325.0 E	
Granite de Porz-Scarff							
HFA	5/8		195.2/+69.8	53.2	10.6	13.4 N, 347.6 E	
HFB	6/6		134.6/+49.2	43.1	10.3	1.3 S, 34.8 E	
XI	4/4		161.4/+68.3	68.8	11.2	11.6 N, 8.5 E	
HFD	8/12		224.7/+38.3	20.5	12.5	9.1 S, 315.2 E	
HFG	5/6		270.3/+55.1	21.2	17.0	26.2 N, 291.8 E	
Mean	5/7		200.4/+66.0	7.3	30.4	8.8 N, 343.2 E	
Rhyolitic Ignimbrites of Lézardrieux and Rhyolites de St.Germain-le-Gaillard							
HFR	5/5	266/40	183.3/+47.6	5.4	36.3	12.5 S, 353.9 E	
VI	4/5	266/40	211.9/+25.0	14.0	25.4	21.9 S, 323.2 E	
HFU	14/22	262/50	189.6/+38.4	9.6	12.2	18.9 S, 347.5 E	
HFIII	5/9	220/72	215.8/+26.1	6.8	31.6	19.9 S, 319.8 E	
HFIV	5/5	238/41	180.8/+49.2	6.4	32.8	11.1 S, 356.2 E	
HFV	6/6	242/32	178.6/+52.6	3.1	46.1	8.1 S, 358.2 E	
a	4/5	242/32	147.6/+24.5	5.7	42.1	4.0 S, 21.1 E	
VBB	6/6	224/90	214.8/+24.5	82.1	7.4	20.5 S, 321.7 E	
Mean	8/8		191.8/+38.2	12.5	16.3	16.1 S, 343.1 E	0.95
Rhyolitic Ignimbrite of Lézardrieux (high-temperature direction at site HFU)							
HFU	9/22	262/50	88.8/-37.1	5.1	25.3	14.7 N, 281.7 E	

N/N_0 is the ratio of samples (sites) used to compute the mean to the total number of samples (sites) analysed; k_1 and k_2 are the Fisher precision parameters before and after correction for the tilt of the strata, respectively; strike and dip denote the bedding attitude of the stratified rocks; α_{95} is the semi-angle of the cone of confidence at the 95 per cent probability level.

a standard field device and magnetic compass, and, weather permitting, a solar compass. Error in orientation is considered at most ± 2° for samples drilled and ± 4° for handsamples. The handsamples were cored at the State University of Utrecht, the Netherlands, to conform with the field drilled diameter of 2.5 cm. The samples were then cut to a specimen length of approximately 2.2 cm.

Natural remanent magnetization (NRM) measurements were made using a PDP-8 computer-assisted Schonstedt DSM-1A Magnetometer at the University of Rennes, France. Stepwise alternating field and thermal demagnetizations were performed on all samples at The University of Michigan. For the granites, spilites, rhyolites and weakest diorites, measurements were made with a Super-Conducting Technology 1½ inch Cryogenic Magnetometer, and for the gabbros and remaining diorites, a Schonstedt SSM-1A Magnetometer was used. Thermal demagnetizations were accomplished with either a Schonstedt Thermal Demagnetizer or by a non-magnetic furnace placed within the field-free space provided by a Helmholtz coil and Schonstedt HCM-3 Triaxial Coil Control Magnetometer feedback system capable of maintaining a field of 5–10 nT or less. For alternating field (AF) demagnetizations up to 100 mT (1000 Oe) a Schonstedt GSD-1 AC Demagnetizer was used. Demagnetization data were plotted using Zijderveld (1967) diagrams and the components of magnetization were resolved by vector subtraction. The directions of magnetization are summarized in Table 1; further details are given in Hagstrum (1979).

Results

Spilites de Paimpol and microgranite dykes

The spilites de Paimpol were sampled at twelve sites across a broad monocline trending east–west (Fig. 1). The tilting of the flows is thought to be due to the Cadomian (Latest Precambrian) orogeny. The exposures sampled at each site comprise several individual spilite flows which, due to well developed pillow structures, are difficult to be identified separately. Hence, the mean magnetic direction for the spilites is calculated from site means, not from individual flow means. At five sites (HFH, HFI, HFJ, 4, 8) microgranite dykes cut the flows and at three sites (HFH, HFI, HFJ) these were also sampled.

A Rb/Sr whole rock isochron dates eruption of the spilites at 640 ± 12 Myr (recalculated with $\lambda = 1.42 \times 10^{-11}$ yr^{-1} from the age given by Vidal 1976). A K/Ar date obtained by the University of Rennes for the dykes yields a minimum age of 510–515 Myr; petrologic affinities with the granite de Porz-Scarff and other microgranite dykes with a Rb/Sr whole rock isochron age of 557 ± 16 Myr suggests that this age is too young by about 9 per cent (Auvray 1975).

In situ NRM directions for both the spilite flows and the microgranite dykes are to the south, south-west or west with shallow to steeply positive inclinations. Initial intensities exhibit a wide range from 10^{-1} to 10^{-4} Am^{-1} (10^{-4} to 10^{-7} emu cm^{-3}).

Thermal and AF demagnetizations were performed on the flows and dykes. Although producing similar directions, each technique had its own set of difficulties. With alternating fields an anhysteretic remanent magnetization (ARM) component became increasingly

---

Figure 2. Orthogonal demagnetization projections (Zijderveld 1967) of the successive endpoints of the magnetization vector during progressive demagnetization, before correction for the tilt of the strata. A thermal (a) and an alternating field demagnetization (b) are shown for specimens of the same sample from a spilite flow remagnetized by a dyke. The diagram in (c) gives another AF demagnetization from a spilite sample which was not remagnetized. Solid circles represent projections on to the horizontal plane, and open symbols those on the north–south vertical plane.

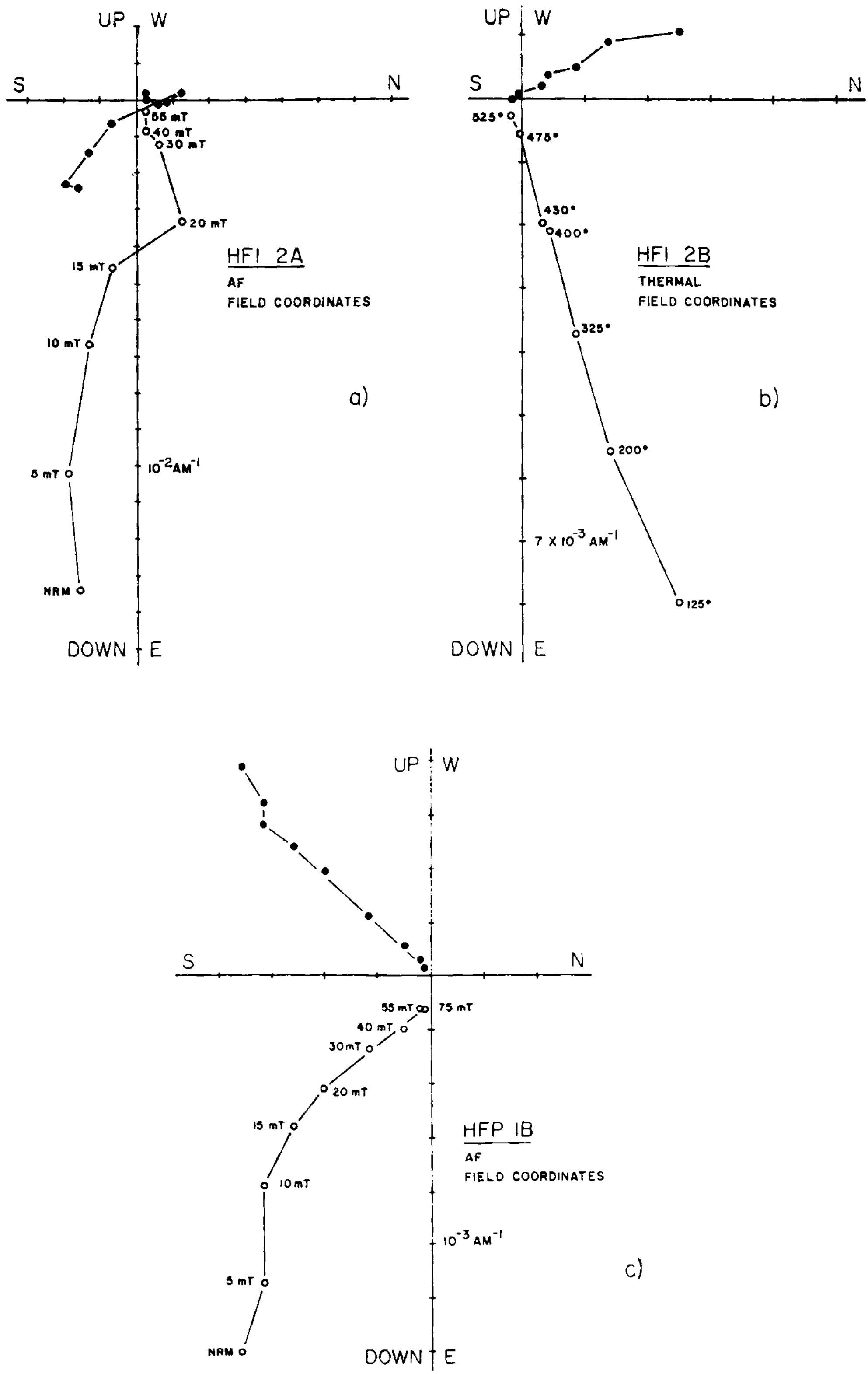
UP W
S
N
55 mT
40 mT
30 mT
20 mT
15 mT
10 mT
5 mT
NRM
HFI 2A
AF
FIELD COORDINATES
a)
10^{-2} AM^{-1}
DOWN E
UP W
S
N
525°
475°
430°
400°
325°
200°
125°
HFI 2B
THERMAL
FIELD COORDINATES
b)
7 X 10^{-3} AM^{-1}
DOWN E
UP W
S
N
55 mT
75 mT
40 mT
30 mT
20 mT
15 mT
10 mT
5 mT
NRM
HFP 1B
AF
FIELD COORDINATES
10^{-3} AM^{-1}
c)
DOWN E

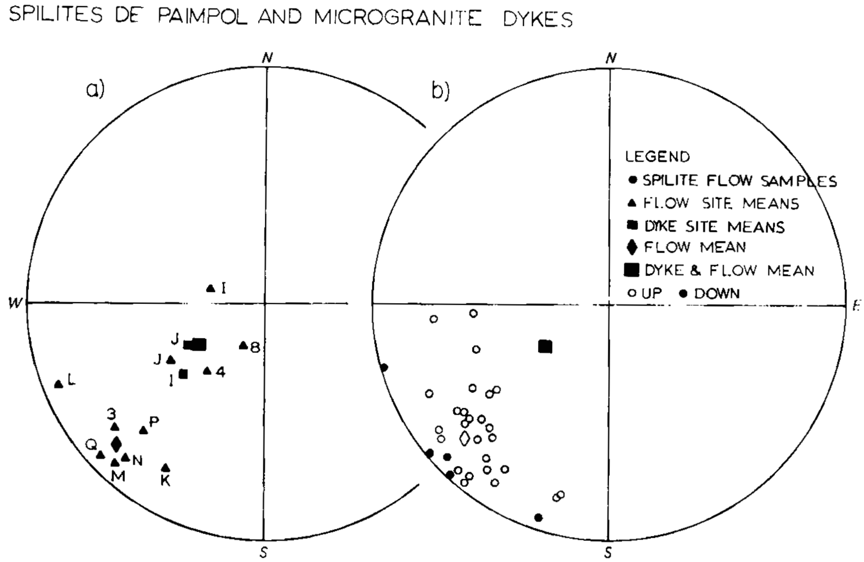

Figure 3. Equal-area projection of the characteristic directions obtained from the spilite flows, the intruding microgranite dykes and from those flows remagnetized by the dykes. (a) Site means before correction for the tilt of the strata; the 'Dyke and Flow mean' includes only remagnetized flows (large square). (b) Characteristic directions obtained from the unremagnetized spilite samples, after correction for the tilt of the strata; the 'Dyke and Flow mean' remains uncorrected. Open (solid) symbols represent projections on to the upper (lower) hemisphere.

troublesome above 30 mT. Also, some samples showed coercivities above the peak field of the AF demagnetizer (100 mT). The major problem with thermal demagnetization was an apparent change in mineralogy above 550°C causing large increases in intensity usually when little of the original magnetization remained in the sample. In many instances, measurement was hampered by a small viscous remanent magnetization (VRM) component induced by the Earth's field during specimen transfer from furnace to magnetometer.

Employing predominantly thermal techniques, soft components of inconsistent orientation were removed below 300°C (or 20 mT in AF demagnetization). Decay of the remaining magnetization was usually univectorial and towards the origin, being eliminated for the most part by 565°C (Fig. 2). Occasionally the vertical and horizontal components of the vector diagram (Zijderveld 1967) converged on a point other than the origin, possibly due to the presence of very small unresolvable magnetizations residing in small high blocking-temperature magnetite grains or hematite, e.g. Fig. 2(b, c). Polished thin sections of the spilites show them to be heavily altered with no magnetic minerals discernable.

Excluding the nearly random directions from site HFH, all flow samples, taken from sites where the microgranite dykes were observed to cut the flows, show a characteristic direction similar to the fairly scattered characteristic components of the microgranite dyke samples (Fig. 3a). The other spilite flows, however, yield a mean characteristic direction of $D = 226.1°, I = +15.4°$ ($\alpha_{95} = 10°, N = 7$ sites) before unfolding (Fig. 3a).

Unfolding the spilite flows (Fig. 3b) results in k_2/k_1 (ratio of the Fisher (1953) precision parameter of the group mean before unfolding to that of the group mean after unfolding) lower than 1.0, which indicates a slightly negative fold test, but insignificant at the 95 per cent confidence level (McElhinny 1964). Such a result was expected due to the uniformity of the tilt correction. For the dykes, the correction has no effect on the dispersion of the magnetic directions.

Because the directions of the flows sampled near the dykes and the directions of the dykes themselves are very similar, it appears that the dykes have locally remagnetized the spilite flows. The pole position defined for the *in situ* magnetization of the dykes and the nearby remagnetized flows is 16.2° N, 310.3° E, and is thought to represent the field at 557 ± 16 Myr ago. We assume the magnetization of the spilite flows away from the dykes to be original and pre-folding, giving a pole position at 33.8° S, 297.2° E. The fact that the microgranite dykes remagnetized only part of the flows supports our contention that the magnetization of the unaffected flows is certainly older than the age of the dykes.

Diorite de St Quay

Seven sites were sampled along the coastal exposure of the gabbroic pluton referred to as the diorite de St Quay (Vidal 1976; Fig. 4). A Rb/Sr isochron determined the age of formation for the diorite at 583 ± 40 Myr – recalculated with $\lambda = 1.42 \times 10^{-11}\ \mathrm{yr}^{-1}$ from the age given by Vidal (1976).

Two or three components of magnetization were found to reside in the diorite samples upon demagnetization. As was the case with the spilites, an ARM component of increasing intensity was acquired with increasing peak alternating fields above 20 mT. The AF peak field did not completely eliminate the magnetization. The thermal technique was used therefore for most of the samples, and though there were sometimes abrupt increases in intensity above 580°C, the method appeared to best resolve the components of magnetization.

The NRM directions exhibited steep inclinations and high intensities ($10^{-1}\ \mathrm{Am}^{-1}$). A large soft component of scattered high inclinations, primarily responsible for the scatter of NRM directions, was sometimes removed by 300°C or 20 mT. Another, better defined component of $D = 299.9°$, $I = +38.2°$ ($\alpha_{95} = 11.5°$, $N = 3$ sites) was removed at intermediate blocking temperatures and coercivities, mostly below 400°C and always below 560°C and 40 mT (Fig. 5). The final characteristic component of $D = 31.2°$, $I = -2.3°$ ($\alpha_{95} = 4.0°$, $N = 7$ sites) was eliminated above these temperatures and coercivities (Fig. 5), but was at times obscured

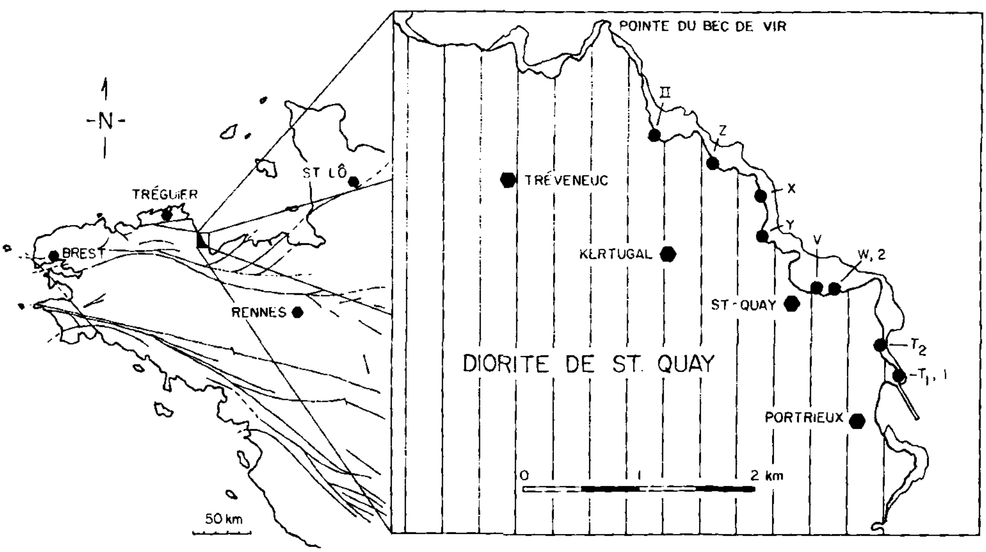

Figure 4. Sampling localities for the diorite de St Quay, northern Brittany.

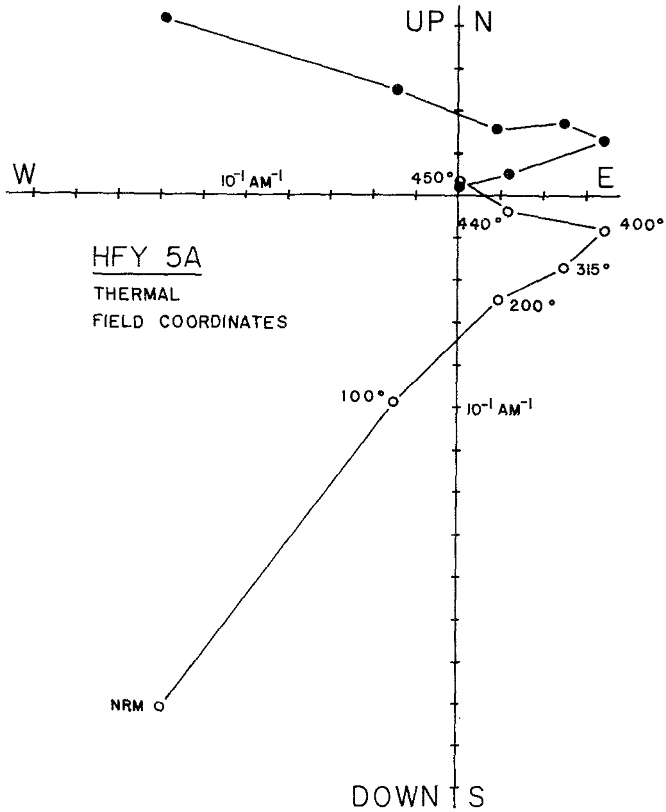

Figure 5. Thermal demagnetization diagram (as in Fig. 2) of a diorite sample exhibiting multivectorial behaviour with both the secondary direction (removed between 20° and 400°C) and the characteristic direction (400° to 450°C) present. Projection on to the east–west vertical plane for greater clarity.

by instrument noise, ARMs, or by possible mineralogy changes. The two components (Fig. 6) were found separately or together in an individual sample.

Polished thin sections were made from samples taken from three sites. The mineralogy appears relatively fresh and original. Large (up to 800 μm) anhedral magnetite grains are oxidized with minor amounts of hematite present. Intergrowths of ilmenite within the magnetite as well as single discrete grains of ilmenite (*c*. 24 μm) were observed. Finer-grained magnetite (down to 5 μm) was found locked within plagioclase and alkali feldspar promising good magnetic stability (Wu, Fuller & Schmidt 1974).

A pole position of 33.7° N, 138.6° E, is calculated for the diorite; we assume that this pole represents the primary magnetization of the intrusion. The intermediate blocking-temperature component yields a pole at 37.6° N, 262.1° E; we infer this magnetization to be secondary. In view of its large size, we assume that the pluton, which intruded into an already stabilized terrane, has not been tilted significantly.

Gabbro de Keralain

From one large ($120 \times 50\,m^2$) site (HFS) and a small site (VII) in the Keralain gabbro stock, and from a site (HFO) in gabbroic dykes just to the south, 37 samples were collected (Fig. 1). Another site (HFE) was taken across the southern contact zone between the gabbro

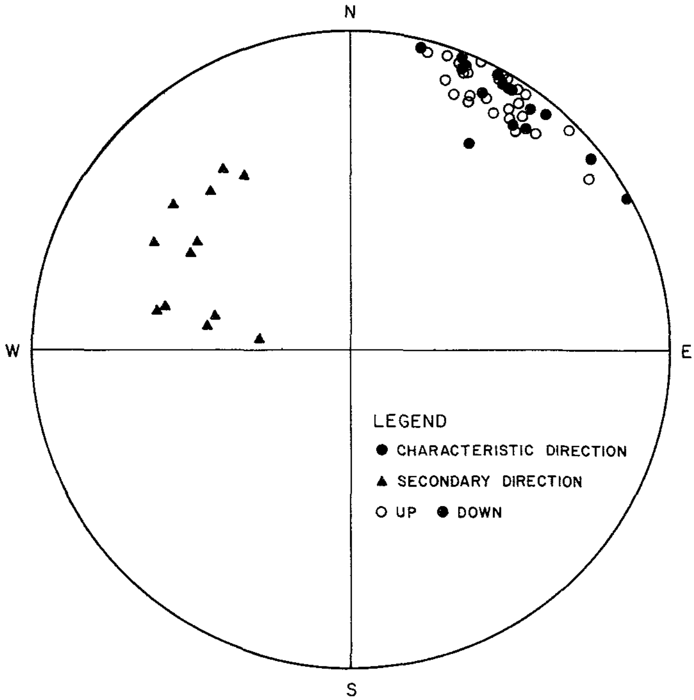

Figure 6. Characteristic and secondary directions of magnetization obtained from the diorite samples in equal-area projection.

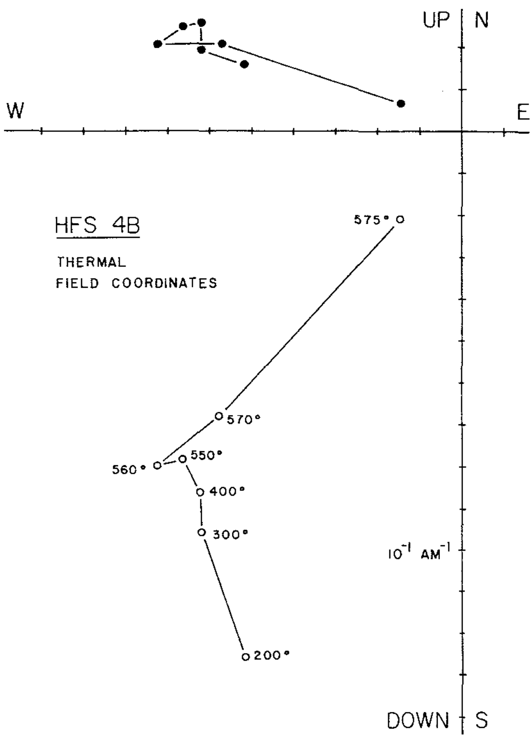

Figure 7. Thermal demagnetization diagram of a gabbro sample from Keralain, showing the secondary direction (removed between 200° and 550°C) and the characteristic direction of magnetization (560° to 575°C).

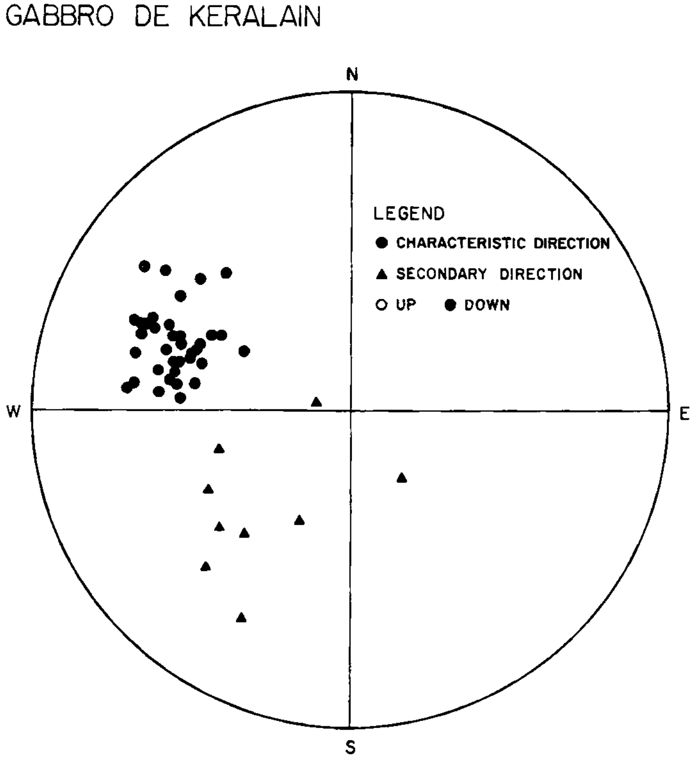

Figure 8. Characteristic and secondary directions of magnetization obtained from the gabbro samples, in equal-area projection.

body and a Late Precambrian keratophyre in the hope of establishing a baked contact test. Unfortunately, no reliable radiometric date could be obtained for the gabbro itself because of an insufficient amount of Rb.

Thermal and alternating field techniques were used in demagnetization of the gabbro giving consistent results between the two methods. Thermal steps were used almost exclusively, however, because a significant portion of the magnetization resided in grains with coercivities greater than the 100 mT peak field limit of the AF demagnetizer.

NRM directions, except for those with very high inclinations (> +70°), are similar to the characteristic directions isolated from the samples. Intensities are relatively high (10^{-1}–10^{-2} Am^{-1}). In the case of site HFE the NRM directions are widely scattered and intensities are low (10^{-3}–10^{-4} Am^{-1}).

As was the case with the diorite de St Quay, two or three components of magnetization were removed (Fig. 7). The first, a very soft and steep component was removed by 250°C or 20 mT. The intermediate directions removed during demagnetization, by 40 mT and for the most part by 560°C, are shown in Fig. 8 (triangles) and their mean is given in Table 1. The last, characteristic direction for the unit gave an *in situ* mean direction of $D = 290.9°$, $I = +41.4°$ ($\alpha_{95} = 3.3°$, $N = 3$ sites; Fig. 8). This component showed a very rapid decrease in intensity above 570°C and was generally removed by 580°C. The directions for this primary component group very well and closely correspond to the secondary directions removed at intermediate temperatures and coercivities from the diorite de St Quay of $D = 299.9°$, $I = +38.2°$. Site HFE was rejected after demagnetization treatment of several samples proved the magnetization to be completely unstable.

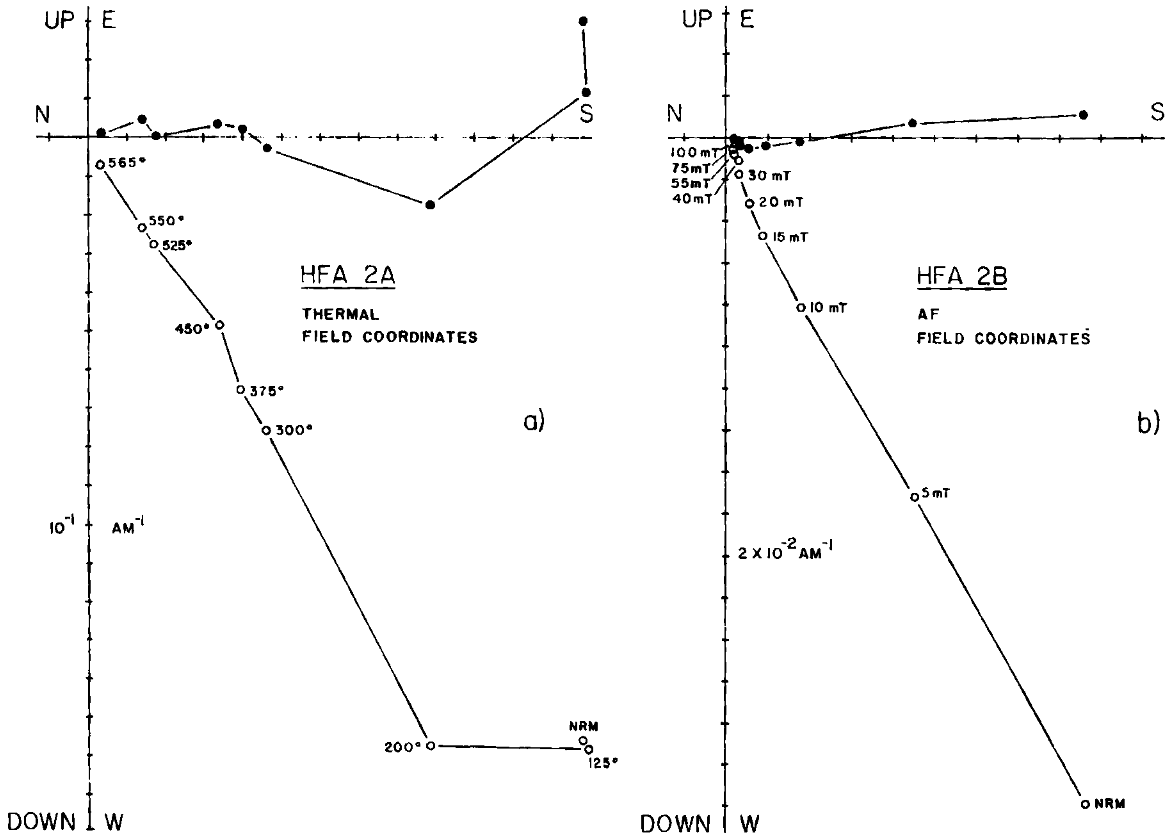

Figure 9. Thermal and AF demagnetization diagrams of two specimens from the same granite sample, showing good agreement in defining the characteristic direction of the granite de Porz-Scarff.

Polished thin sections reveal coarse magnetite grains (50 μm) which are only slightly oxidized. Large chalcopyrite grains (up to 320 μm) are present with replacement rims 25 μm thick of chalcocite. Some finer grained opaques (*c.* 10 μm) consist of pyrite and ilmenite, but most likely the carrier of the magnetic components is magnetite which is too fine-grained to be recognized optically.

The pole for the high blocking-temperature gabbro magnetization is 31.3° N, 268.3° E. Since the gabbro is a relatively small intrusive body, the question could be raised as to whether the body has been tilted. The observed mean direction, however, agrees well with other directions observed in the Armorican Massif (to be discussed later) and we see no reason to assume a significant tilting of the intrusive.

Granite de Porz-Scarff

The granite de Porz-Scarff was sampled at seven sites around the perimeter and towards the centre of the pluton (Fig. 1). Radiometric dating (Rb/Sr whole rock isochron technique) gives a date of 557 ± 16 Myr for the intrusion and cooling of the granite – recalculated with $\lambda = 1.42 \times 10^{-11}\ \mathrm{yr}^{-1}$ from the age given by Vidal (1976).

The samples exhibited primarily a univectorial decay upon demagnetization by both thermal and alternating field methods (Fig. 9). Most samples were processed thermally to avoid ARM problems above 30 mT. Directions isolated for the samples were relatively scattered overall, but quite consistent within sites (Fig. 10). Such was also the case with the NRM directions. Initial intensities ranged from 1 to $10^{-4}\ \mathrm{Am}^{-1}$. The granite's magnetization was primarily removed at temperatures below the Curie point for magnetite (578°C) giving a mean direction of $D = 200.4°$, $I = +66.0°$ (Table 1) which is similar to the secondary direction removed from the gabbro de Keralain of $D = 221.0°$, $I = +55.8°$. The resulting pole position for the granite is 8.8° N, 343.2° E. One site, HFC, showed a univectorial component which persisted above 580°C up to the Néel point of hematite (680°C). NRM

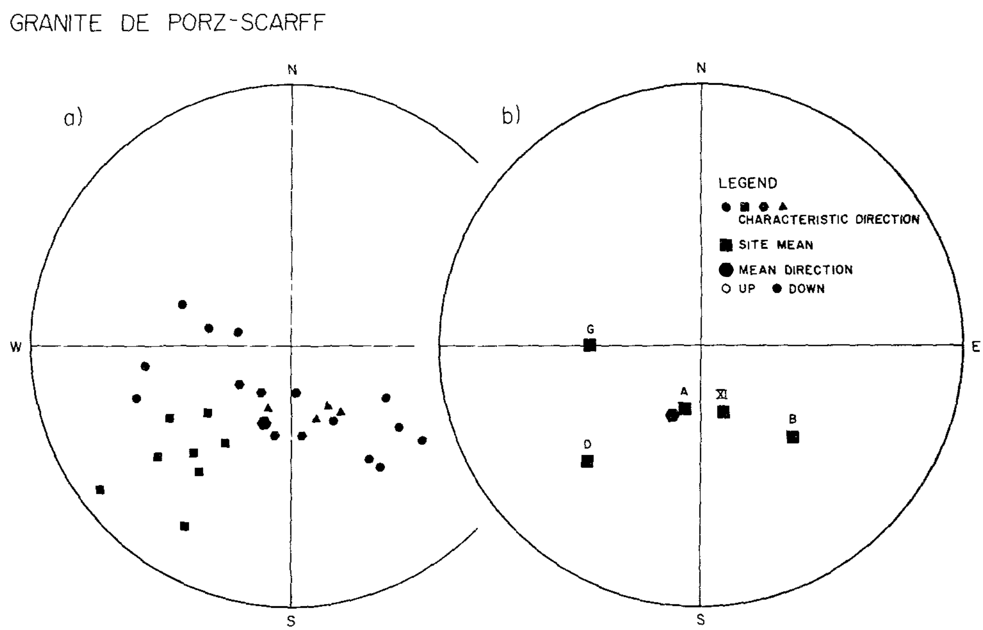

Figure 10. Equal-area projections of the directions of magnetization obtained from the granite. (a) Sample directions, each site denoted by a distinguishing symbol. (b) Site-mean directions and overall mean direction of the granite.

results for this site included the abnormally high intensities of 1 Am^{-1} and widely scattered directions similar to the scatter of the demagnetized positions ($\alpha_{95} = 62.6^\circ, N = 5$ samples). Both the NRM and demagnetization results are in disagreement with the general trend for the other sites and therefore the results of site HFC were discarded. One other site was omitted from the formation mean: site HFF, while exhibiting well behaved demagnetizations, yielded scattered, inconsistent directions ($\alpha_{95} = 67.5^\circ, N = 6$ samples).

The granite from sites HFA, HFC, HFF and HFG, in polished thin section appears to be heavily altered. Coarse grains of magnetite (50 μm) have been 80 per cent oxidized to hematite. Secondary hematite was also found in very small grains (10 μm) after biotite. Occasionally fine-grained (*c.* 10 μm) magnetite was also seen. The rejected sites HFC and HFF showed only small diameter grains of hematite with a minor amount of magnetite present, possibly indicating a higher degree of weathering at these two sites.

We believe the characteristic magnetization of the granite to be primary because it appears to reside mostly in the original portions of the magnetite grains.

Rhyolitic ignimbrites of Lezardrieux and rhyolites de St Germain-le-Gaillard

The results of the rhyolitic ignimbrites of Lézardrieux of Brittany (Fig. 1) and their sampled counterparts, the rhyolites de St Germain-le-Gaillard (St G-le-G) of Normandy (Fig. 11), are difficult to interpret because of two problems: a lack of knowledge about the need to apply a correction for the tilt of the strata and some ambiguities about their age(s). Measurement of possible bedding attitudes was made for each site (and for each of the 22 samples of site HFU) on the basis of the eutaxitic structures; it is entirely possible, however, that these structures represent primary extrusive/intrusive features.

Published Rb/Sr dating at one of our sites places the age of the ryolitic ignimbrites of Lézardrieux at 547 ± 12 Myr – recalculated with $\lambda = 1.42 \times 10^{-11}\ yr^{-1}$ from the age given by Vidal (1976), whereas the rhyolite de St G-le-G is considered to be Latest Precambrian

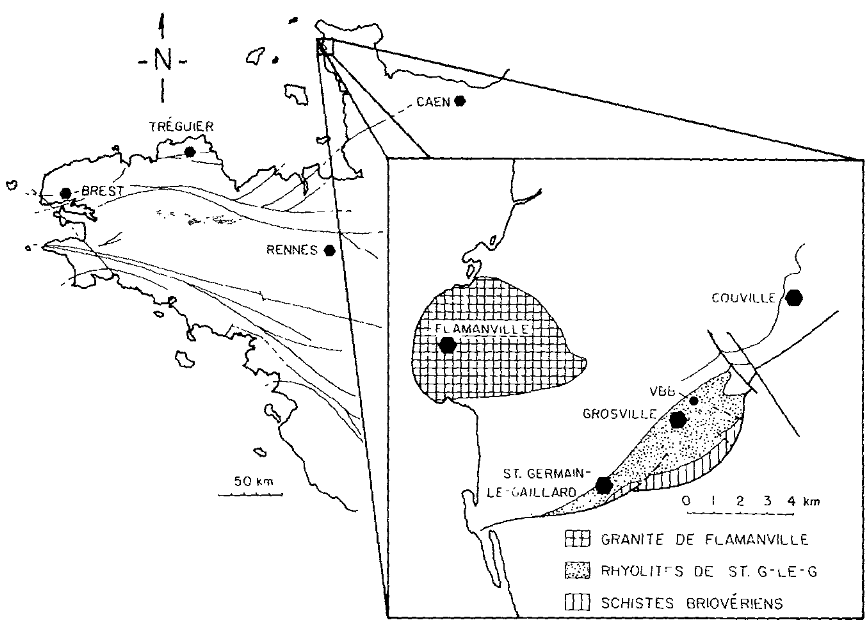

Figure 11. Map of the sampling locality for the rhyolites de St Germain-le-Gaillard, in the Domnonean Domain (northern Normandy).

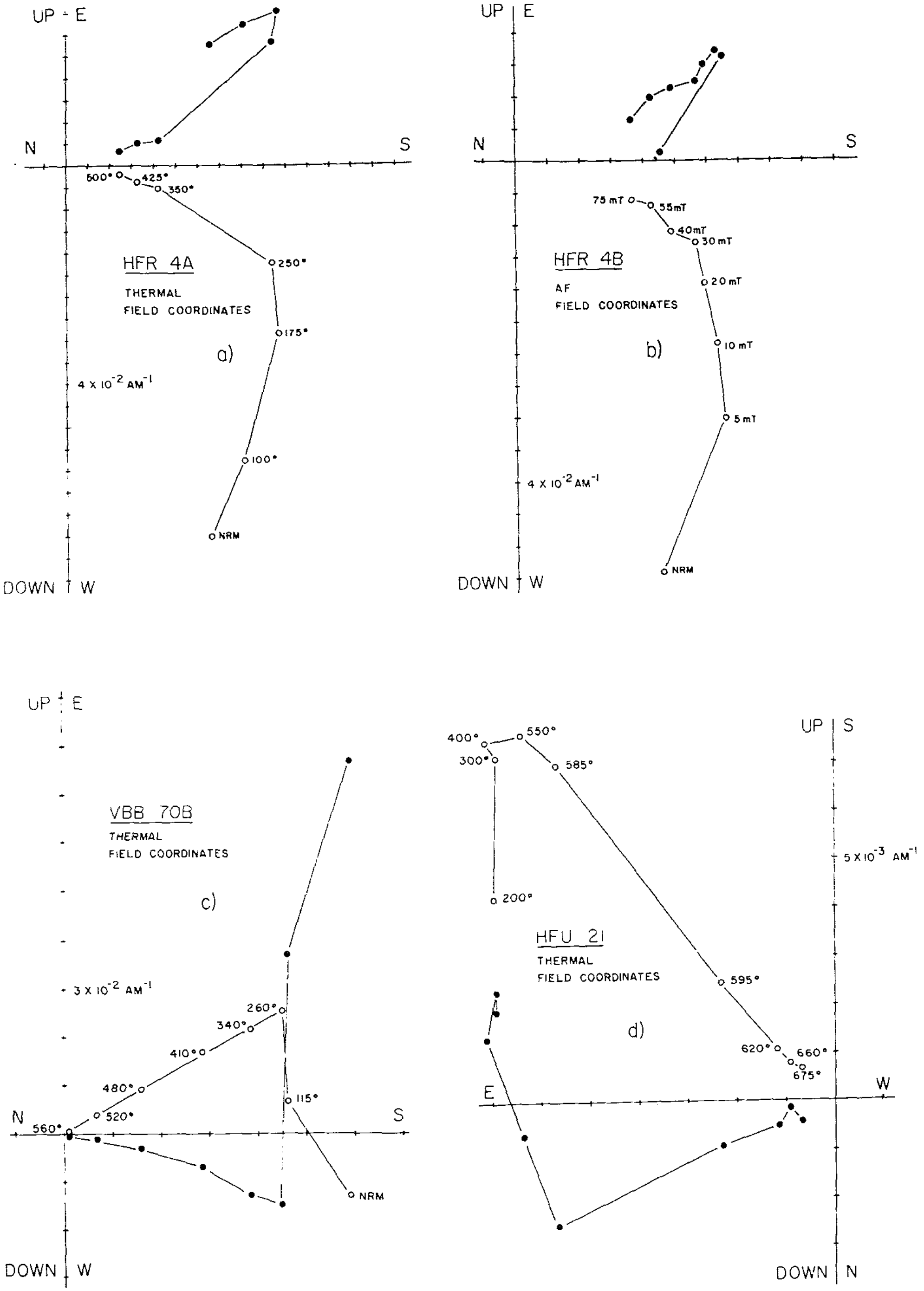

Figure 12. Thermal and AF demagnetization diagrams for samples from the rhyolitic ignimbrites of Lézardrieux: (a) and (b) two specimens of the same sample showing agreement between the two methods; (c) thermal demagnetization of a sample from the rhyolites de St Germain-le-Gaillard, and (d) a thermal demagnetization of a sample from site HFU which contains the characteristic component (removed between 400° and 550°C) and a high-temperature component (585° to 675°C) seen only at this site of Les Héaux; note that the plot in (d) is plotted along different axes for clarity.

Table 2. Rb/Sr whole rock isochron analyses of the rhyolitic ignimbrites of Lézardrieux.

Site(s)	Age (MA)	Number of samples
Les Héaux (HFU)	531 ± 34	3
La Roche Donan (HFR, VI)	589 ± 14	3
Le Tour de Kerroc'h (HFIII,HFIV,HFV,a)	547 ± 12	6
Les Héaux + La Roche Donan	567 ± 11	6
Les Héaux + La Roche Donan + Le Tour de K.	546 ± 8	12

to Middle Cambrian in age (Boyer, Roblot & Graindor 1972). Although the rhyolitic ignimbrites appear uniform petrologically, there is somewhat of a dispersion in newly obtained Rb/Sr whole rock measurements from three localities (Fig. 1: sites R; III, IV, V; and U). This indicates that the possibility exists that one (or all) of these widespread rhyolitic localities is not co-magmatic with the others. With permission of J. Macé of the geochronology laboratory at the University of Rennes we reproduce here the main isochron results of their work, for individual localities as well as their overall result (Table 2). In addition, we note that rhyolitic volcanism, almost everywhere shown to be of Cambrian age (Boyer 1968), is widespread in Brittany, Normandy and the Channel Islands. With the exception, however, of the occurrence in the Island of Jersey (Duff 1978a; 522 ± 16 Myr, recalculated with $\lambda = 1.42 \times 10^{-11}\,\text{yr}^{-1}$), these other rhyolites are not radiometrically dated.

NRM directions were widely scattered because of the presence of secondary magnetizations and intensities were low (10^{-2}–$10^{-4}\,\text{Am}^{-1}$). Thermal techniques appeared to most clearly define the characteristic magnetization of the rhyolites by best removing the scattered secondary component when present. Nevertheless, similar results were obtained from AF demagnetization (Fig. 12). The secondary components were usually eliminated by 400°C or 30 mT, leaving the characteristic component with a mean *in situ* direction of $D = 182.1°$, $I = +2.0°$ (rhyolites de St G-le-G included). For site HFU there remained different high-temperature components up to 675°C (e.g. Fig. 12d) with a mean *in situ* direction of $D = 54.8°$, $I = -33.2°$ ($\alpha_{95} = 15.1°$, $N = 9$ samples) above the blocking temperatures for magnetite (Fig. 13). On the other hand, high-temperature directions (above 600°C) observed in samples from site HFR were similar to the lower blocking-temperature directions (below 580°C).

Polished thin sections from site HFU contain abundant fine-grained hematite (< 30 μm diameter) in replacement after biotite, amphibole and magnetite. Coarser grained hematite (up to 100 μm) shows relic euhedral textures indicating complete replacement of original magnetite grains. No magnetite is visible in these slides from site HFU which showed both the characteristic and high-temperature north-easterly directions. Polished sections from the other sampled rhyolitic bodies show predominantly magnetite in varying stages of oxidation. In site HFR samples, abundant grains of magnetite are seen ranging in size from 5 to 320 μm which are 15–20 per cent oxidized along rims and cracks to hematite. The biotite and amphibole grains for site HFR appear relatively intact. This site showed only characteristic directions, but with blocking temperatures below and above 580°C. Rhyolites from site VBB (St G-le-G) and sites HF III and HF V (Le Tour de Kerroc'h) contain magnetite (in a similar size distribution as that of site HFR) with the coarse magnetite, biotite and amphibole phenocrysts being more oxidized (magnetite: *c.* 80 per cent or more) than the finer grains (< 25 μm) which are more angular in shape and fresher in appearance. The oxidation at this site could be a high-temperature (deuteric) process associated with the emplacement

RHYOLITES DE LÉZARDRIEUX AND RHYOLITES DE ST. GERMAIN-LE-GAILLARD

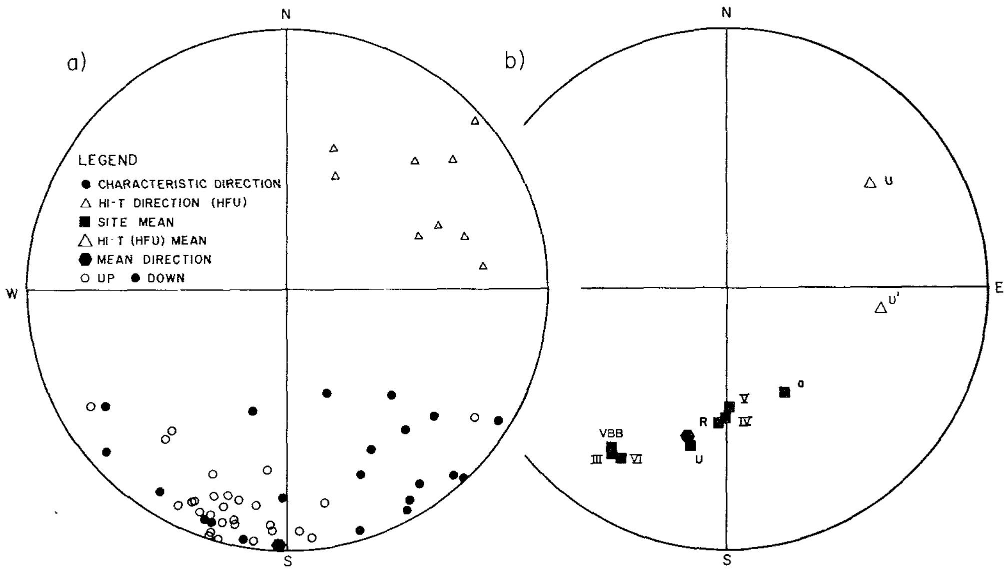

Figure 13. (a) Characteristic directions for all rhyolites and the high-temperature directions from site HFU (triangles); (b) site-mean directions corrected for the tilt of the strata and the high-temperature mean direction before (U) and after correction for tilt (U′). Lambert equal-area projections.

and cooling of the rhyolites as evidenced by the involvement of the biotite and amphibole phenocrysts.

Applying the tilt correction to the rhyolites does not give a positive fold test for the overall characteristic direction observed at all sites, nor for the high-temperature direction seen only at site HFU. This suggests that either the rhyolites acquired their magnetization post-'folding', or that some of the applied corrections are wrong, or that the eutaxitic structure is a primary structure which is not genetically horizontal. The validity of basing a bedding correction on the attitude of the eutaxitic structure was brought into serious question when the structure was seen to vary from horizontal to near vertical in a single albeit fairly large block of rhyolite. At site VBB the rhyolites were intercalated with sedimentary units defining a clear tilt correction there, whereas the tilt correction was the most poorly defined at La Roche Donan (sites HFR, VI), where the best possible correction returns the eutaxitic structure to approximately vertical and not the horizontal. Whether this indicates an intrusive rather than extrusive nature at this site can not be decided without further study.

We prefer to consider the characteristic direction of magnetization as primary, but of limited value. The characteristic direction for the rhyolites after unfolding (Table 1) yields a pole position of 16.1° S, 343.1° E. Tentatively, this pole is assigned an (Eo?)-Cambrian age of 546 ± 8 Myr. There does not seem to be a significant difference between the directions from the three widespread localities of Les Héaux, Le Tour de Kerroc'h, or St G-le-G (Figs 1 and 11), so that separate ages (Table 2) and separate poles do not appear to be warranted. Until more results from rhyolitic bodies in other areas are obtained, however, we prefer not to attach equal significance to this pole, when constructing an apparent polar wander path, in view of the uncertainties about structural tilt and the different possibilities for the ages of the rhyolites. The high-temperature direction seen only at site HFU could have originated in Cambrian or later times, and cannot be decisively interpreted at the present time.

Discussion

Within the data there appears a trend in magnetization and partial remagnetization of the magnetite grains in the units consistent with their radiometric dates. The oldest unit, the Spilites de Paimpol (640 ± 12 Myr), gives a direction (D/I = 226.4°/– 15.7°) not far from that of the diorite de St Quay (D/I = 211.2°/+2.3°, taking the opposite polarity), the next youngest (583 ± 40 Myr) unit of the collection. The diorite also shows a secondary direction (D/I = 299.9°/+38.2°) that is equivalent to the primary direction (D/I = 290.9°/+41.4°) of the undated gabbro de Keralain which itself gives a secondary direction (D/I = 221.0°/ 55.8°) close to the primary direction of the granite de Porz-Scarff (D/I = 200.4°/+66.0°). Thus, we are able to date the gabbro as having been emplaced after 583 Myr (age of the diorite) and before 557 Myr (age of the granite). The direction–age association of the granite is again substantiated by the microgranite dykes, which cut and locally remagnetize the spilites, with a minimum K/Ar age (510–515 Myr) and direction (D/I = 235.1°/+63.4°) close to that of the granite (D/I = 200.4°/+66.0°). The rhyolitic ignimbrites of Lézardrieux (546 ± 8 Myr) and the rhyolites de St G-le-G give after unfolding a more tentative direction (D/I = 191.8°/+38.2°) near to that of the granite, consistent with the contention (Auvray 1975) that the granite, microgranite dykes and rhyolites are all from the same Late Precambrian–Early Cambrian phase of acidic volcanism. We consider the characteristic direction of the rhyolites less reliable than those of the other units on the basis of the uncertainty in the tilt correction and in the radiometric dating. Also, the possibility of complete remagnetization is enhanced due to the unclear nature of the separate high-temperature direction.

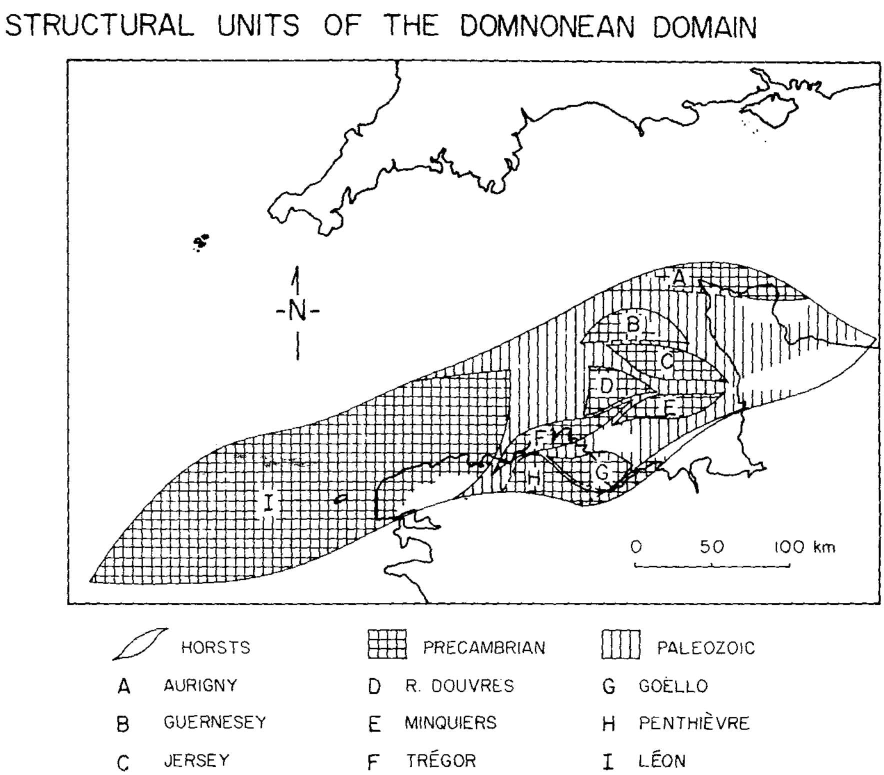

Figure 14. Schematic depiction of the structural units of the Domnonean Domain of the Armorican Massif (after Lefort 1965).

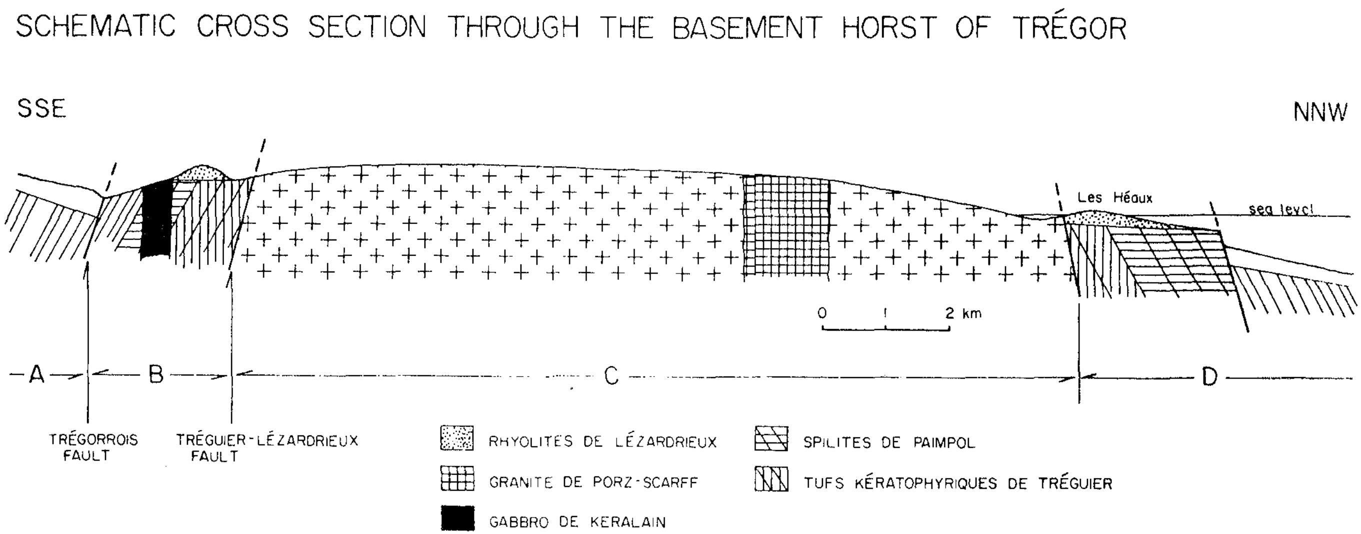

Figure 15. Schematic cross section through the Trégor horst passing through Les Héaux and Paimpol (see Fig. 1 for location). Both the Gabbro de Keralain and the Granite de Porz-Scarff have been projected on to the section along the general strike. A: Belt of Plourivo-Plouézec with Cambro–Ordovician redbeds and volcanics unconformably overlying sedimentary formations of the Upper Brioverian (Jones *et al.* 1979). B: Belt of Tréguier–Paimpol, with Cambrian rhyolites unconformably overlying schists, graywackes, spilites and keratophyric tuffs of the Upper Brioverian. C: basement of Trégor consisting of a granitic–granodioritic complex, including slices of Pentevrian gneiss and important systems of microgranite and dolerite dykes. D: immergent northern flank of the Trégor Horst with Cambrian rhyolites unconformably overlying spilites and tuffs of the Upper Brioverian, separated from Eocene and Devonian sediments to the north by faults (after Fig. 5 from Auvray *et. al* 1976b).

The Domnonean Domain, as shown in Fig. 14, can be divided into a number of small separate structural units. Rotations or tilting between these units would disperse the declinations and inclinations of the palaeomagnetic data from them (i.e. Trégor, Goëllo – this study; Jersey – Duff 1978b; Guernsey – Hailwood & Garrett 1977). However, the relative motion between the above mentioned blocks appears to be primarily dip-slip in nature and small in magnitude, implying that the error from these movements for our purposes is not very significant (Cogné 1971, 1974; Lefort 1975).

Fig. 15 shows a cross-section of our field area (le Trégor) from NNW to SSE across the uplifted basement block and the flanking Late Precambrian–Cambrian sedimentary and volcanic units. K/Ar age dating from the basement horst gives an age of 630 Myr (Vidal 1976), suggesting that it has not been subjected to a thermal event exceeding 300°C since this time. A Late Cambrian–Early Ordovician (472 ± 5 Myr, Rb/Sr whole rock isochron date) trachyandesite sampled by Jones, Van der Voo & Bonhommet (1979) to the south of the Trégorrois fault does give a reset K/Ar age of 345 Myr. This Hercynian thermal episode to the south appears not to have affected the adjacent volcanic and sedimentary belt of Tréguier–Paimpol since the included microgranite dykes give a K/Ar age of at least 510–515 Myr. This radiometric evidence supports our conclusion that the characteristic magnetizations observed for the units of this study are magnetizations of at least Cambrian age or older. In addition, there are petrologic and palaeomagnetic considerations that indicate the magnetizations to be primary. These are, in arbitrary order:

(1) Magnetite is the prevailing magnetic mineral in most rock types studied and appears to be primary in thin sections;

(2) the microgranite dykes remagnetized only those parts of the spilites into which they intruded, indicating that the magnetization of the spilites is older than that of the dykes;

(3) rocks of approximately the same age give similar directions;

(4) despite the similarity of the directions of the diorite de St Quay to Permo-Carboniferous directions elsewhere in Europe, the observed polarity of the diorite is opposite the prevailing Permo-Carboniferous polarity during the Kiaman interval;

(5) the presence of lower-temperature directions, assumed to be secondary and correlating with characteristic directions of other younger rock units, suggests a primary origin for their higher-temperature directions insofar as they are also carried by magnetite.

Implications from these and other studies

All reliable palaeomagnetic data from the Armorican Massif and other parts of Europe within the time period from Latest Precambrian to Late Cambrian (*c.* 650–500 Myr) have been compiled in Table 3 and the pole positions have been plotted in Fig. 16. A tentative path indicating the approximate polar wander for the Armorican Massif has been drawn in Fig. 16(a), to best fit the poles and their succession of radiometric or stratigraphic ages. This trend is corroborated by the sequence of poles from the diorite ($SQ_1 \rightarrow SQ_2$), gabbro ($GK_1 \rightarrow GK_2$), and granite–microgranite–rhyolite sequence (MI → MR → PS), discussed in the previous section. In addition, results of the St Peter Port Gabbro of Guernsey (Hailwood & Garrett 1977), which was intruded by the Bordeaux Diorite, follow the sequence of poles ($PP_{1\text{-}2} \rightarrow PP_3$). Younger, Cambrian poles for the Armorican Massif have been obtained by Duff (1978b) from the island of Jersey (poles JV, SEG, SWG and NWG). It should be noted that the last two poles of the path (RB and RM: Table 3, Fig. 16a), believed to be valid for the Late (?) Cambrian of the Armorican Massif, are among the least certain of all the poles, because they are based on high-temperature directions observed in only a small number of samples (Jones 1978). However, the samples of pole RB yielded good quality demagnetizations with directions passing a fold test at the 95 per cent confidence level and showing both normal and reversed polarities.

Palaeomagnetic poles from southern United Kingdom and from Czechoslovakia (Table 3), poor by comparison, are plotted in Fig. 16(b). It is possible, although at present quite

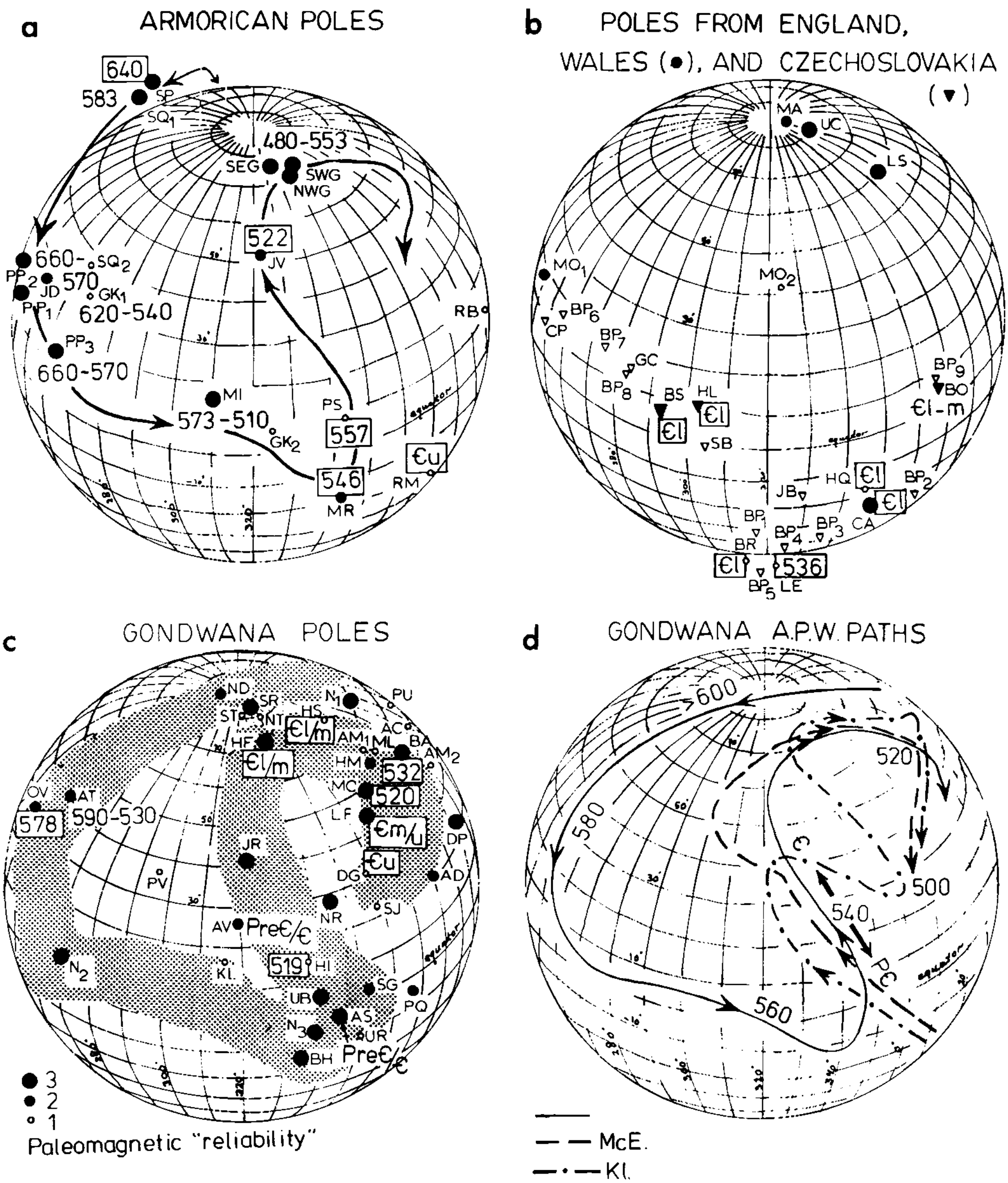

Figure 16. Palaeomagnetic pole positions for the Eocambrian–Cambrian (650–500 Myr) as listed in Tables 3 and 4. Palaeomagnetic reliability indicated by size of symbol (after McElhinny & Embleton 1976); age control indicated by radiometric or stratigraphic age in rectangle ('3'), without rectangle ('2'), or not indicated at all ('1'). (a) Poles from the Armorican Massif, (b) poles from the southern United Kingdom and from Czechoslovakia (Table 3), (c) poles from the reassembled Gondwana continents (Table 4), and (d) three possible polar wander paths through these poles from McElhinny & Embleton (1976), Klootwijk (private communication, 1978), and this study, with approximate ages indicated in Myr and the Precambrian–Cambrian boundary assumed at *c.* 550 Myr.

speculative, to draw an apparent polar wander path through these poles, similar to that defined by the Armorican data, in particular if one only considers the most reliable results (larger, closed symbols). Critical for this comparison between the Armorican Massif and the southern United Kingdom is the pole obtained by Duff (1978b) for the Leicester Diorites (pole LE). This pole position (63° S, 321° E) is based on only three sites (two other sites gave poles at 68° N, 34° E and at 52° N, 303° E), but the age of the complex, recalculated with $\lambda = 1.42 \times 10^{-11}\ \text{yr}^{-1}$ from the age given by Cribb (1975), appears to be very reliable. The pole of the Leicester Diorites does not fall on the apparent polar wander path of Fig. 16, nor does its antipole. However, assuming that only the most reliable poles are valid for the Eocambrian–Cambrian of southern United Kingdom and Czechoslovakia, it is not inconceivable that these areas behaved as a single continental mass together with the Armorican Massif. All three have very similar geological histories and a common Latest Precambrian orogeny (Cadomian or Assyntian orogeny: Stille 1924). This continental mass is here called the Armorica plate, and existed in Latest Precambrian and Early Palaeozoic time.

A comparison of poles and apparent polar wander paths between Armorica and Gondwana (assembled in a pre-drift configuration) is also possible. Gondwana poles are compiled in Table 4, and are plotted in Fig. 16(c). Since the data are somewhat sketchy, various interpretations of the polar wander path are possible. Three alternative interpretations are illustrated in Fig. 16(d). The dashed line is that of McElhinny & Embleton (1976); the dot and dash line is that of Klootwijk (private communication); the solid line is a modification of that by Kröner *et al.* (1980) preferred by the authors. At first glance the three paths look very different even though they are all more or less based on the same poles. The main difference between the paths of McElhinny & Embleton and of Klootwijk is the extra loop in the Middle Cambrian to include poles LF and AD. Both paths use the antipoles of the older (> 550 Myr) data, so the primary differences between their paths and ours are in the way poles OV and BH are connected (see Fig. 16d), and in the inclusion of the $N_1 \rightarrow N_2 \rightarrow N_3$ pole sequence in the proper order as proposed by Kröner *et al.* (1980).

Table 3. Eocambrian–Cambrian pole positions from Europe (650–500 Myr).

Symbol	Rock unit	Age	(control)	Pole position (reliability)	Reference
BALTIC SHIELD AND RUSSIAN PLATFORM					
FC	Fen Carbonatite	600-530	(1)	63N, 142E (1)	14/425
AB	Asha series, Basinsk Group	573	(3)	8N, 189E (3)	Irving et al.(1976):2/108
AK	Asha series, Kukkaraukian	590-573	(1)	11N, 147E (0)	Irving et al.(1976):2/169
NE	Nexø Sandstone, Denmark	PreꞒ/Ꞓ	(1)	38N, 134E*(3)	Prasad & Sharma (1978)
				* recalculated	from original
SOUTHERN ENGLAND AND WALES					
MO_1	Mona Complex, Gwna	c.600	(2)	17N, 237E (2)	15/227
LD	Dykes in Longmyndian (redated as Silurian)			not plotted	Lomax & Briden (1977)
MO_2	Mona Complex, in situ NRM	Ꞓ ?	(0)	42N, 324E (0)	Lomax (1975)
LE	Leicestershire Diorites	539-533	(3)	63N, 141E (1)	Duff (1978 b)
MA	Malvernian, in-situ	Ꞓ ?	(0)	86N, 56E (2)	Lomax & Briden (1977)
UC	Uriconian, in-situ	Ꞓ ?	(0)	80N, 41E (3)	Lomax & Briden (1977)
LS	Longmyndian sediments, in-situ	Ꞓ	(1)	60N, 29E (3)	Lomax & Briden (1977)
BR	Bangor redbeds	Ꞓ1	(3)	54N, 132E (0)	Duff (1978 b)
CA	Caerfai series	Ꞓ1	(3)	26N, 169E (3)	13/66
HQ	Hartshill quartzite	Ꞓ1	(3)	18N, 165E (1)	5/83

Table 3 – *continued*

Symbol	Rock unit	Age	(control)	Pole position (reliability)		Reference
ARMORICAN MASSIF, FRANCE						
SP	Spilites, Paimpol	640±12	(3)	34S, 297E	(3)	this study
SQ_1	Diorite, St.Quay	583+40	(2)	34S, 319E	(3)	this study
PP_1	St.Peter Port Gabbro, in-situ	660-570	(2)	14N, 237E	(3)	Hailwood & Garrett (1977)
PP_2	St.Peter Port G., dip-corrected	660-570	(2)	13N, 224E	(3)	Hailwood & Garrett (1977)
PP_3	Bordeaux Diorite contact in PP	660-570	(2)	13N, 263E	(3)	Hailwood & Garrett (1977)
JD	Jersey C-Dolerite dykes	PreC/Є ?	(0)	26N, 248E	(2)	Duff (1978 b)
GK_1	Gabbro, Keralain	620-540	(2)	31N, 268E	(1)	this study
SQ_2	Diorite St.Quay, secondary	PreC/Є?	(0)	38N, 262E	(1)	this study
MI	Microgranite dykes & contacts	573-510	(2)	16N, 310E	(3)	this study
GK_2	Gabbro Keralain, secondary	PreЄ/Є?	(0)	8N, 325E	(1)	this study
PS	Granite, Porz-Scarff	557±16	(3)	9N, 343E	(2)	this study
MR	Mainland rhyolites	546± 8	(2)	16S, 343E	(2)	this study
JV	Jersey volcanics	522±16	(3)	52N, 323E	(2)	Duff (1978 b)
NWG	Northwest Granite, Jersey	480 ?	(2)	73N, 353E	(3)	Duff (1978 b)
SWG	Southwest Granite, Jersey	553 ?	(2)	74N, 356E	(3)	Duff (1978 b)
SEG	Southeast Granite, Jersey	509 ?	(2)	77N, 337E	(3)	Duff (1978 b)
RB	Redbeds, Zone Bocaine	Є	(1)	9N, 45E	(1)	Jones (1978)
RM	Redbeds, Syncline of May	Єu	(3)	23S, 15E	(1)	Jones (1978)
BOHEMIAN MASSIF, CZECHOSLOVAKIA						
BP_1	Barrandian Porphyry E	PreЄ/Є	(1)	32N, 136E	(0)	5/86
BP_2	Barrandian Porphyry F	PreЄ/Є	(1)	30N, 185E	(0)	5/86
BP_3	Barrandian Porphyry D	PreЄ/Є	(1)	40N, 156E	(0)	5/86
BP_4	Barrandian Porphyry C	PreЄ/Є	(1)	52N, 147E	(0)	5/86
BP_5	Barrandian Porphyry A3	PreЄ/Є	(1)	66N, 134E	(0)	5/88
JB	Jince Beds	Є	(2)	16N, 149E	(1)	8/140
CP	Czech. Porphyrites	Є	(2)	10N, 248E	(0)	8/139
BP_6	Barrandian Porphyry A2	PreЄ/Є	(1)	17N, 255E	(0)	5/88
BP_7	Barrandian Porphyry A4	PreЄ/Є	(1)	17N, 274E	(0)	5/88
GC	Glubshsky Conglomerate	PreC/Є	(1)	14N, 283E	(1)	8/141
BP_8	Barrandian Porphyry A1	PreЄ/Є	(1)	13N, 282E	(0)	5/88
BS	Barrandian sediments	Єl	(3)	7N, 294E	(3)	Krs & Vlašímský (1976)
HL	Hlubos and Sadek beds	Єl	(3)	10N, 302E	(2)	8/146
SB	Sadecky beds	PreЄ/Є	(1)	1S, 305E	(0)	8/142
BP_9	Barrandian Porphyry B	Є	(2)	9N, 6E	(0)	5/87
BO	Bogutinsky Sandstone	Єl-m	(2)	8N, 7E	(2)	8/143

Symbols correspond to Fig. 16. Age control is based on the following criteria (3 = radiometric age or stratigraphic age known within half-period (*c.* 30 Myr) limits, 2 = age known within period (*c.* 50 Myr) limits, 1 = age known within approximately 120 Myr; 0 = age not known, but inferred). Pole position reliability from McElhinny & Embleton (1976), with 3 being the most reliable ($A_{95} < 15°$, at least four sites, 15 samples, and result based on stability test). Reference numbers refer to the Palaeomagnetic pole lists of McElhinny (1968a, 1972a, b) and McElhinny & Cowley (1977, 1978) and the pole list of Irving (1964).

The Armorican and Gondwana apparent polar wander paths – (Fig. 16a and c) – display a remarkable similarity. We propose therefore that during the Latest Precambrian and the Cambrian the two plates were coupled and moved together, relatively juxtaposed as they are

Table 4. Eocambrian–Cambrian palaeomagnetic pole positions from the Gondwana continents (650–500 Myr).

Symbol	(Continent)	Rock unit	Age	(control)	Pole Position	(reliability)	Rotated ("AF") Pole	Reference
ND	(AF)	Pre-Nama dykes	653±70	(1)	85N, 228E	(2)	85N, 228E	14/530
SR	(AF)	Sabaloka Ring Structure	>540	(0)	83N, 339E	(3)	83N, 339E	quoted in Piper et al. (1973)
N_1	(AF)	Lower Nama Group	700-600	(1)	62N, 61E	(3)	62N, 61E	Kröner et al. (1980)
PQ	(AU)	Pound Quartzite	L.PreЄ	(1)	60S, 6E	(2)	5S, 6E	14/564
BH	(IN)	Bhander sandstone	PreЄ/Є	(1)	49S, 33E	(3)	15S, 335E	14/424
UR	(IN)	Upper Rewa sandstone	PreЄ/Є	(1)	35S, 42E	(1)	11S, 350E	14/514
UB	(IN)	Upper Bhander sandstone	PreЄ/Є	(1)	32S, 19E	(3)	4N, 339E	14/515
AS	(AU)	Arumbera/Todd River	PreЄ/Є	(2)	45S, 340E	(3)	3S, 344E	Kirschvink (1978)
SG	(AF)	Sijarira Group	PreЄ/Є	(1)	2N, 352E	(2)	2N, 352E	12/149
NR	(AF)	Ntonya Ring Structure	630-570	(1)	28N, 345E	(3)	28N, 345E	9/137
KL	(AF)	Klipheuvel Formation	PreЄ/Є	(1)	16N, 316E	(1)	16N, 316E	Creer (1973)
AV	(AU)	Antrim volcanics	PreЄ/Єl	(2)	9S, 340E	(2)	26N, 319E	12/148
N_2-FR	(AF)	Upper Nama (Fish River)	PreЄ/Є	(1)	5N, 271E	(3)	5N, 271E	Kröner et al. (1980)
OV	(AF)	Ouarzazate volcanics	578±15	(3)	30N, 237E	(2)	30N, 237E	Hailwood & Tarling (1973)
AT	(AF)	Amouslek Tuffs	590-530	(2)	41N, 250E	(2)	41N, 250E	Hailwood & Tarling (1973)
PV	(SA)	Purmamarca Village	Є	(1)	61N, 293E	(1)	36N, 295E	14/420
AD	(AU)	Aroona Dam sediments	PreЄ/Єl	(2)	36S, 33E	(2)	21N, 20E	14/416
N_3	(AF)	Nama Grp., secondary	PreЄ/Є	(1)	7S, 337E	(3)	7S, 337E	Kröner et al. (1980)
JR	(AF)	Jordanian Redbeds	Є-O	(0)	37N, 323E	(3)	41N, 321E	12/147
HF	(AU)	Hudson Formation	Єl/m	(3)	18N, 19E	(3)	72N, 338E	14/413
ST	(SA)	South Tilcara	Є	(1)	52N, 27E	(1)	82N, 329E	14/417
NT	(SA)	North Tilcara	Є	(1)	49N, 23E	(1)	80N, 350E	14/418
HS	(AU)	Hugh River Shale	Єl/m	(3)	11N, 37E	(1)	68N, 33E	14/415
ML	(AF)	Moroccan lavas	Єl-m	(?)	53N, 34E	(1)	53N, 34E	Helsley (1965)
BA	(AF)	Bou Azzer Volcs, sed's.	532±18	(3)	47N, 42E	(3)	47N, 42E	Daly & Pozzi (1976)
LF	(AU)	Lake Frome Group	Єm/u	(3)	14S, 24E	(3)	43N, 8E	14/409
DP	(AF)	Doornpoort, secondary	<550	(0)	22N, 45E	(3)	22N, 45E	14/529
DG	(AU)	Dundas Group	Єu	(3)	23S, 13E	(1)	31N, 358E	15/226
PU	(SA)	Purmamarca	Є	(1)	5N, 39E	(1)	45N, 80E	14/421
AC	(SA)	Abra de Cajas	Є	(1)	2N, 28E	(1)	41N, 66E	14/419
SJ	(SA)	Salta & Jujuy	Є-O	(0)	12N, 329E	(1)	22N, 358E	12/146
MC	(AN)	Mirnyy Charnockites	520±24	(2)	2N, 208E	(3)	49N, 14E	14/408
HM	(AF)	Hasi-Messaud sediments	Є-O	(0)	53N, 26E	(2)	53N, 26E	15/141
HI	(AF)	Hook Intrusives	519±17	(3)	14N, 336E	(1)	14N, 336E	9/132
AM_1	(AF)	Adrar de Mauritanie, CO_{10}	Є/O	(1)	55N, 30E	(1)	55N, 30E	Morris & Carmichael (1978)
AM_2	(AF)	Adrar de Mauritanie, CO_8	Є/O	(1)	36N, 52E	(0)	36N, 52E	Morris & Carmichael (1978)

Symbols correspond to those of Fig. 16. Age control and palaeomagnetic reliability as in Table 3. The rotated ('AF') pole position corresponds to the pole in pre-drift coordinates with respect to the African continent. Reference numbers as in Table 3.

today. Before 580 Myr ago, one could argue that the two paths are different, since the Armorica poles SP and SQ_1 are quite different from those of Gondwana. Insufficient data precludes speculation if this implies a Late Precambrian (Cadomian?) convergence. More certain, on the other hand, is the conclusion that during the Palaeozoic the Armorica and Gondwana plate must have separated, since by Late Devonian time the two are far apart and separated by an ocean (Jones *et al.* 1979). Judging from the rather poor Ordovician and Silurian data for Gondwanaland, and comparing these with contemporaneous poles for Armorica (United Kingdom and Czechoslovakia), a Late Cambrian/Ordovician separation is permitted but by no means proven by the data.

A tentative interpretation of the movements of these continental masses and North America is presented in palaeolatitude reconstructions for the Latest Precambrian and the Middle Cambrian (Fig. 17). Throughout this time period Gondwanaland is apparently undergoing a counter-clockwise rotation relative to North America which remains essentially fixed (Watts 1979). Simultaneously, Armorica is moving with Africa from intermediate to

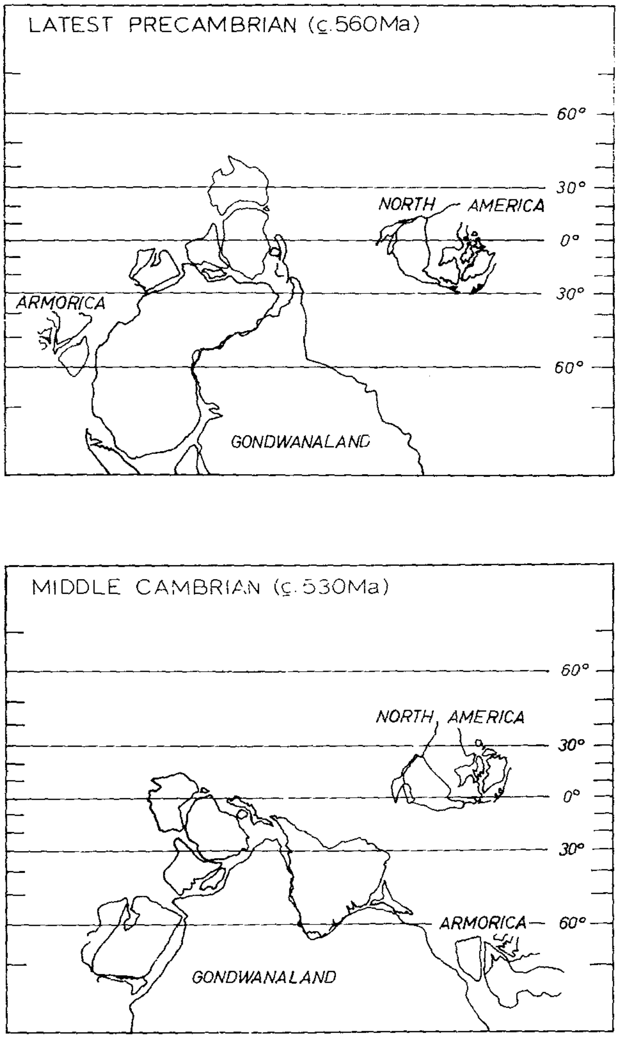

Figure 17. Mercator palaeolatitude reconstructions based on Latest Precambrian poles (UB, AS, BH, AV) and Middle Cambrian poles (LF, AD) of Table 4 for Gondwana, as well as on poles listed by Elston & Bressler (1977), Van der Voo, French & Williams (1976), and Watts (1979) for North America.

high latitudes and back to intermediate latitudes in the southern hemisphere. The earlier Late Precambrian (*c.* 600 Myr) convergence of the Armorica and Gondwana plates may be correlated with the Cadomian orogeny which is recognized in the Armorican Massif and elsewhere in western Europe (Stille 1924; Rutten 1969; Cogné 1971, 1974; Vidal 1976; Duff 1978b) as responsible for extensive deformation, plutonism and subsequent angular unconformities between the Late Precambrian (Brioverian) clastic series and the transgressive base of the Cambrian (Rutten 1969).

The separation of Armorica and Gondwana, possibly in Late Cambrian or Ordovician time, has important implications for subsequent orogenies in the Palaeozoic. The Armorica plate may be thought of as an individual continental entity at the outset, and recognized for the role that it may have played in the tectonic framework of the Caledonian and Hercynian orogenies.

Acknowledgments

The authors would like to thank Dr Rex E. Crick of The University of Michigan for his critical examination of the manuscript, Dr J. D. A. Zijderveld of the State University of Utrecht for the use of their laboratory, and Mr John W. Geissman for his evaluation of the polished thin sections.

This study forms part of an extensive palaeomagnetic program, jointly undertaken by The University of Michigan and the CNRS laboratory ('Centre Armoricain d'Etude Structurale des Socles') of the University of Rennes. Financial support for this work came from the Division of Earth Sciences, the National Science Foundation, grant EAR 76-14996, and in part from the Scott Turner Fund, Department of Geology and Mineralogy, University of Michigan.

References

Auvray, B., 1975. Relations entre plutonisme acide et volcanisme ignimbritique; example des manifestations magmatiques Cambriennes du Nord de la Bretagne, *Pétrologie*, t. **1**, 125–138.

Auvray, B., Lefort, J. P. & Monnier, J. L., 1976a. Carte Géologique de la France au 1/50,000, feuille VIII-14 Tréguier, *Service Géologique National.*

Auvray, B., Lefort, J. P. & Monnier, J. L., 1976b. Notice explicative feuille VIII-14 Tréguier, *Service Géologique National*, 26 pages.

Badham, J. P. N. & Halls, C., 1975. Microplate tectonics, oblique collisions, and the evolution of the Hercynian Orogenic systems, *Geology*, **3**, 373–376.

Boyer, Cl., 1968. Sur la nature ignimbritique de certaines porphyroides du Massif Armoricain et du Massif Central, *C. r. Acad. Sci. Paris*, **266** (D), 1464–1466.

Boyer, Cl., Roblot, M. M. & Graindor, M. J., 1972. Les ignimbrites du Post-Briovérien de Saint Germain-le-Gaillard (Manche), *C. r. Acad. Sci. Paris*, **247** (D), 21–33.

Burne, R. V., 1973. Palaeogeography of south west England and Hercynian continental collision, *Nature Phys. Sci.*, **241**, 129–131.

Burrett, C. F., 1972. Plate tectonics and the Hercynian Orogeny, *Nature Phys. Sci.*, **239**, 155–157.

Cogné, J., 1971. Le Massif Armoricain et sa place dans la structure des socles Ouest-Européens: l'arc Hercynien Ibéro-Armoricain, in *Histoire Structural du Golfe de Gascogne*, vol. 1, pp. 1–23, Publication de l'institut français du pétrole, collection colloques et séminaires, 22, Editions Technip, Paris.

Cogné, J., 1974. Le Massif Armoricain, in *Géologie de la France*, ed. Debelmas, J., vol. 1, pp. 106–161, Doin Editeurs, Paris.

Creer, K. M., 1973. A discussion of the arrangement of palaeomagnetic poles on the map of Pangaea for epochs in the Phanerozoic, in *Implications of Continental Drift to the Earth Sciences*, eds Tarling, D. H. & Runcorn, S. K., vol. 1, pp. 47–76, Academic Press, London.

Cribb, S. J., 1975. Rubidium–strontium ages and strontium isotope ratios from the igneous rocks of Leicestershire, *J. geol. Soc. London*, **131**, 203–212.

Daly, L. & Pozzi, J. P., 1977. Determinations d'un nouveau pole paléomagnétique africain sur des formations Cambriennes du Maroc, *Earth planet. Sci. Lett.*, **34**, 264–272.

Dewey, J. F. & Burke, K. C. A., 1973. Tibetan, Variscan, and Precambrian basement reactivation: products of continental collision, *J. Geol.*, **81**, 683–692.

Dewey, J. F. & Kidd, W. S. F., 1974. Continental collisions in the Appalachian–Caledonian orogenic belt: variations related to complete and incomplete suturing, *Geology*, **2**, 543–546.

Duff, B. A., 1978a. Rb–Sr whole-rock age determination of the Jersey Andesite formation, Jersey, C.I., *J. Geol. Soc. London*, **135**, 153–156.

Duff, B. A., 1978b. Palaeomagnetic and rock magnetic studies of lower Palaeozoic rocks on Jersey and the adjacent regions of the Armorican Massif, *PhD thesis*, University of Leeds.

Elston, D. P. & Bressler, S. L., 1977. Paleomagnetic poles and polarity zonation from Cambrian and Devonian strata of Arizona, *Earth planet. Sci. Lett.*, **36**, 423–433.

Fisher, R. A., 1953. Dispersion on a sphere, *Proc. R. Soc. Lond. A*, **217**, 295–305.

Floyd, P. A., 1972. Geochemistry, origin and tectonic environment of the basic and acidic rocks of Cornubia, England, *Proc. Geol. Assoc.*, **83**, 384–404.

French, R. B., 1976. Lower paleozoic paleomagnetism of the North American craton, *PhD thesis,* University of Michigan, Ann Arbor.

Hagstrum, J. T., 1979. Eocambrian–Cambrian paleomagnetism of the Armorican Massif, France, *MSc thesis,* University of Michigan, Ann Arbor.

Hailwood, E. A. & Garrett, C., 1977. Palaeomagnetism, and the dynamothermal history of the St Peter Port Gabbro, Guernsey, *Proc. Ussher Soc.,* 4, 26–35.

Hailwood, E. A. & Tarling, D. H., 1973. Palaeomagnetic evidence for a proto-Atlantic ocean, in *Implications of Continental Drift to the Earth Sciences,* eds. Tarling, D. H. & Runcorn, S. K., vol. 1, pp. 37–46, Academic Press, London.

Helsley, C. E., 1965. Paleomagnetic results from the Middle Cambrian of north-west Africa, *Trans. Amer. geophys. Un.,* **46**, 67.

Irving, E., Tanczyk, E. & Hastie, J., 1976. Catalogue of paleomagnetic directions and poles, third issue: Paleozoic results 1949–1975, Geomagnetic Service of Canada, *Ottawa, Geomagnetic Series,* **5**, 98 pages.

Irving, E., 1977. Drift of the major continental blocks since the Devonian, *Nature,* **270**, 304–309.

Johnson, G. A. L., 1973. Closing of the Carboniferous sea in western Europe, in *Implications of Continental Drift to the Earth Sciences,* eds Tarling, D. H. & Runcorn, S. K., vol. 2, pp. 843–850, Academic Press, London.

Johnson, G. A. L., 1974. Crustal margins and plate tectonics during the Carboniferous, in *C. R. 7th Intern. Congress Carboniferous Stratigraphy and Geology,* Krefeld (1971), Band III, pp. 261–265.

Jones, M., 1978. Paleozoic paleomagnetism of the Armorican Massif, France, *MSc thesis,* University of Michigan, Ann Arbor.

Jones, M., Van der Voo, R. & Bonhommet, N., 1979. Late Devonian to Early Carboniferous paleomagnetic poles from the Armorican Massif, France, *Geophys. J. R. astr. Soc.,* **58**, 287–308.

Kirschvink, J. L., 1978. The Precambrian–Cambrian boundary problem: paleomagnetic directions from the Amadeus Basin, Central Australia, *Earth planet. Sci. Lett.,* **40**, 91–100.

Kröner, A., McWilliams, M. O., Germs, G. J. B., Reid, A. B. & Schalk, K. E. L., 1980. Paleomagnetism of Late Precambrian to Early Paleozoic mixtite-bearing formations in Namibia (SW Africa): (I) the Nama Group and Blaubeker Formation, *Am. J. Sci.,* in press.

Krs, M. & Vlašímský, P., 1976. Palaeomagnetic study of Cambrian rocks of the Barrandian (Bohemian Massif), *Geofysikální sborník,* **24**, 263–280.

Laurent, R., 1972. The Hercynides of South Europe: a model, *24th Intern. Geol. Congress Montreal,* **3**, 363–370.

Lefort, J. P., 1975. Le socle periarmoricain: étude géologique et géophysique du socle submergé á l'ouest de la France, *Thèse de Doctorat,* University of Rennes.

Lomax, K., 1975. Palaeomagnetic studies of Proterozoic rocks in Britain and West Africa, *PhD thesis,* University of Leeds.

Lomax, K. & Briden, J. C., 1977. Palaeomagnetic studies of the Longmyndian and other British Late Precambrian/Early Palaeozoic rocks, and their regional tectonic implications, *J. Geol. Soc. London,* **133**, 5–21.

Lorenz, V., 1976. Formation of Hercynian subplates: possible causes and consequences, *Nature,* **262**, 374–377.

McElhinny, M. W., 1964. Statistical significance of the fold test in palaeomagnetism, *Geophys. J. R. astr. Soc.,* **8**, 338–340.

McElhinny, M. W., 1968a. Palaeomagnetic directions and pole positions – VIII, *Geophys. J. R. astr. Soc.,* **15**, 409–430.

McElhinny, M. W., 1968b. Palaeomagnetic directions and pole positions – IX, *Geophys. J. R. astr. Soc.,* **16**, 207–224.

McElhinny, M. W., 1972a. Palaeomagnetic directions and pole positions – XII, *Geophys. J. R. astr. Soc.,* **27**, 237–257.

McElhinny, M. W., 1972b. Palaeomagnetic directions and pole positions – XIII, *Geophys. J. R. astr. Soc.,* **30**, 281–293.

McElhinny, M. W. & Cowley, J. A., 1977. Palaeomagnetic directions and pole positions – XIV, *Geophys. J. R. astr. Soc.,* **49**, 313–356.

McElhinny, M. W. & Cowley, J. A., 1978. Palaeomagnetic directions and pole positions – XV, *Geophys. J. R. astr. Soc.,* **52**, 259–276.

McElhinny, M. W. & Embleton, B. J. J., 1976. Precambrian and Early Palaeozoic palaeomagnetism in Australia, *Phil. Trans. R. Soc. Lond. A,* **280**, 417–431.

McKerrow, W. S. & Ziegler, A. M., 1972. Paleozoic oceans, *Nature Phys. Sci.*, **240**, 92–94.

Morel, P. & Irving, E., 1978. Tentative paleocontinental maps for the Early Phanerozoic and Proterozoic, *J. Geol.*, **86**, 535–561.

Morris, W. A. & Carmichael, C. M., 1978. Paleomagnetism of some late Precambrian and lower Paleozoic sediments from l'Adrar de Mauritanie, West Africa, *Can. J. Earth Sci.*, **15**, 253–262.

Nicolas, A., 1972. Was the Hercynian orogenic belt of Europe of the Andean type? *Nature Phys. Sci.*, **236**, 221–223.

Piper, J. D. A., Briden, J. C. & Lomax, K., 1973. Precambrian Africa and South America as a single continent, *Nature*, **245**, 244–248.

Prasad, S. N. & Sharma, P. V., 1978. Palaeomagnetism of the Nexø Sandstone from Bornholm Island, Denmark, *Geophys. J. R. astr. Soc.*, **54**, 669–680.

Pruvost, P., Waterlot, G. & Delattre, C., 1966. 2e édition de la feuille géologique Tréguier au 1/80,000, *Serv. Carte Géol. France.*

Riding, R., 1974. Model of the Hercynian fold belt, *Earth planet. Sci. Lett.*, **24**, 125–135.

Runcorn, S. K., 1962. Palaeomagnetic evidence for continental drift and its geophysical cause, in Continental Drift, *International Geophysical Series*, **3**, pp. 1–40, Academic Press, New York & London.

Rutten, M. G., 1969. *The Geology of Western Europe*, Elsevier, New York.

Stille, H., 1924. *Grundfragen der vergleichenden Tektonik*, Borntraeger, Berlin.

Van der Voo, R., French, R. B. & Williams, D. W., 1976. Paleomagnetism of the Wilberns Formation (Texas) and the late Cambrian paleomagnetic field for North America, *J. geophys. Res.*, **81**, 5633–5638.

Van Eysinga, F. W. B., 1975. *Geologic time table*, 3rd edn, Elsevier, Amsterdam.

Vidal, P., 1976. L'évolution polyorogénique du Massif Armoricain: apport de la géochronologie et de la géochemie isotopique du strontium, *Thèse de Doctorat*, University of Rennes.

Watts, D. R., 1979. Upper Keweenawan and lower Paleozoic paleomagnetism of the North American craton, *PhD thesis*, University of Michigan, Ann Arbor.

Wilson, J. T., 1966. Did the Atlantic close and then re-open? *Nature*, **211**, 676–681.

Wu, Y. T., Fuller, M. & Schmidt, V. A., 1974. Microanalysis of NRM in a granodiorite intrusion, *Earth planet. Sci. Lett.*, **25**, 275–285.

Zijderveld, J. D. A., 1967. AC demagnetization of rocks: analysis of results, in *Methods in Paleomagnetism*, eds Collinson, D. W., Creer, K. M. & Runcorn, S. K., pp. 254–286, Elsevier, New York.